

# Electronic SUPPORTING INFORMATION for Sustainable sorbitol-derived compounds for gelation of the full range of ethanol-water mixtures

Glenieliz C. Dizon,<sup>ab</sup> George Atkinson,<sup>ab</sup> Stephen P. Argent,<sup>a</sup> Lea T. Santu,<sup>ab</sup> and David B. Amabilino\*<sup>ab</sup>

<sup>a</sup> School of Chemistry, University of Nottingham, University Park, NG7 2RD, United Kingdom

<sup>b</sup> The GSK Carbon Neutral Laboratories for Sustainable Chemistry, University of Nottingham, Triumph Road, NG7 2TU, United Kingdom

## Experimental

### Materials and methods

All starting materials and solvents were purchased from standard chemical suppliers: Acros (cuminaldehyde 98%, 4-TSA monohydrate 97.5%, D-sorbitol 97%), Merck (cinnamaldehyde 98%, vanillin 98%), Sigma (vanillin acetate 98%).

**Melting points** were recorded on a Stuart SMP20. **Optical rotations** were recorded using an Anton Paar MCP100 Polarimeter, at 25.0 °C, at a concentration of 10 mg mL<sup>-1</sup>, equipped with a 2.50 mm cell length and  $[\alpha]^{25}_D$  values are given in deg cm<sup>2</sup> g<sup>-1</sup>. **NMR** spectra were recorded on a Bruker Ascend 400. **FTIR** spectra were recorded on a Bruker Alpha Platinum ATR. **Mass Spectra** were obtained using Bruker Compass MicroTOF, using electron spray ionisation (ESI). **CHN Analysis** were obtained using the CE-400 Elemental Analyzer, Exeter Analytical, INC. 1.6 mg of each sample was combusted at temperature 975 °C. **Powder X-Ray diffraction (XRD)** patterns were obtained by the Bruker D8 Advance with Da Vinci. 5 mL of each sample was prepared and were dried under reduced pressure to obtain xerogels. The xerogels were placed on a silicon wafer zero background sample holders for data acquisition in 2-Theta scale between 1 – 65°, with step size of 0.02°, a step time of 6 seconds per step, using parallel beam mode at 40 kV and 40 mA. **X-ray diffraction (XRD)** data were collected in a Rigaku Oxford Diffraction (Rigaku, Tokyo, Japan) at 120(2) K with an Agilent Diffraction microfocus tube with Cu K $\alpha$  radiation type at 1.54184, equipped with an Atlas CCD area detector (S2). **Scanning Electron Microscopy Measurements (SEM)** samples were prepared by dropping a small amount of gel onto a SEM stub with a Pasteur pipette. The samples were left to dry in air overnight to give a xerogel, and then coated with iridium for imaging. For high resolution imaging on an FEG-SEM work, Iridium is the finest grading of coating and is recommended because it produce significantly better results than the other metal coatings. An argon plasma is used in a vacuum chamber to sputter particles of metal from the targets, which form a thin (5 nm) layer on the sample. Images of the xerogels were captured using a JEOL 7100F FEG-SEM microscope. **Rheological measurements** were taken using an Anton Paar Physica MCR 301 rheometer. Samples were

heated to solution and were transferred into a mould on a rheometer plate. Samples were ensured to gel before rheological measurements were taken using a 50 mm cone plate. **Gelation tests** were performed using a Crystallisation Systems Crystal 16. Samples were heated from 20 °C to 80 °C at a rate of 5 °C min<sup>-1</sup>, held at 80 °C for five minutes, and then cooled back to 20 °C at a rate of -5 °C min<sup>-1</sup>. Stirring was carried out on the ramp up at 800 rpm using stirrer bars. No stirring was done during the hold or the ramp down to avoid disturbing any nascent fibres.

### Single crystal X-ray diffraction

Single crystals were selected and mounted using Fomblin® (YR-1800 perfluoropolyether oil) on a polymer-tipped MiTeGen MicroMount™ and cooled rapidly to 120 K in a stream of cold N<sub>2</sub> using an Oxford Cryosystems open flow cryostat.<sup>ESI1</sup> Single crystal X-ray diffraction data were collected on an Oxford Diffraction GV1000 (AtlasS2 CCD area detector, mirror-monochromated Cu-K $\alpha$  radiation source;  $\lambda = 1.54184 \text{ \AA}$ ,  $\omega$  scans). Cell parameters were refined from the observed positions of all strong reflections and absorption corrections were applied using a Gaussian numerical method with beam profile correction (CrysAlisPro).<sup>ESI2</sup> Structures were solved within Olex2<sup>ESI3</sup> by dual space iterative methods (SHELXT)<sup>ESI4</sup> and all non-hydrogen atoms refined by full-matrix least-squares on all unique F<sup>2</sup> values with anisotropic displacement parameters (SHELXL).<sup>ESI5</sup> Hydrogen atoms were refined with constrained geometries and riding thermal parameters. Structures were checked with checkCIF.<sup>ESI6</sup> CCDC- 1945762-1945763 contains the supplementary data for these compounds. These data can be obtained free of charge from The Cambridge Crystallographic Data Centre via [www.ccdc.cam.ac.uk/data\\_request/cif](http://www.ccdc.cam.ac.uk/data_request/cif).

### Crystal structure refinement details

**MBS-Van** The absolute configuration of the structure is determined by reference to the D-sorbitol starting material. Refinement of each configuration gives the same R1 value. Refinement of the opposite configuration gives a lower Flack parameter however this is not significant given the large uncertainty of the refined value.

The crystal was weakly diffracting with a resolution limit of 0.9 Å. The data was truncated to a resolution of 0.9 Å resulting in a low data to parameter ratio, necessitating application of a large number of restraints to the cinnamyl moieties of the two residues (DFIX, DANG and FLAT). Rigid bond restraints were applied to the anisotropic displacement parameters of all atoms in the structure (RIGU).

The cinnamyl moiety of residue B is disordered over two conformations the occupancies of which have been refined and constrained to sum to unity, having values of 0.65(4) and 0.35(4). The anisotropic displacement parameters of the disordered moieties have been restrained to be similar (SIMU). Geometric restraints applied to the 1,2 and 1,3 distances in the disordered moieties were calculated using Grade Web Server v1.104. The

anisotropic displacement parameters of disordered atoms C17C/B and C18C/B have been restrained to have more isotropic character (ISOR).

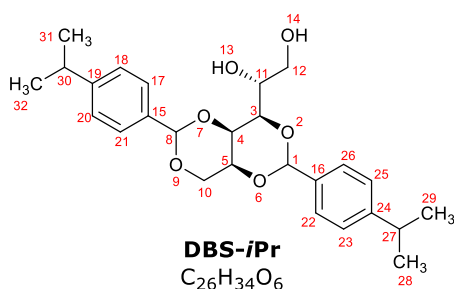
Hydrogen atoms bound to carbon atoms in the structure were geometrically placed and refined using a riding model. Hydroxyl hydrogen atoms were not observed in the electron density map and are geometrically placed to donate hydrogen bonds to appropriate acceptors. Geometric placement of hydroxyl atoms on O4B and O12B clashed with hydrogen atoms of adjacent hydroxyl groups and were omitted from the model. Their correct positions could not be determined from the electron density map and it is likely that many of the hydrogen bonds are in fact disordered with roles of donors and acceptors interchangeable. The omitted hydrogen atoms are included in the unit cell contents.

**MBS-Cinn** Hydrogen atoms attached to carbon atoms were observed in the electron density map before being geometrically placed and refined using a riding model. The positions of hydroxyl-hydrogen atoms H8, H8, H12 and H22 are refined with their O-H bond distances restrained to a target value of 0.84 Å (DFIX). Hydroxyl-hydrogen atom H2 was geometrically placed and refined with a riding model (AFIX 147). The isotropic displacement parameters of the hydroxyl-hydrogen atoms are fixed at a value of 1.5 time Ueq of their parent oxygen atoms.

## Synthetic procedures

### General Methods

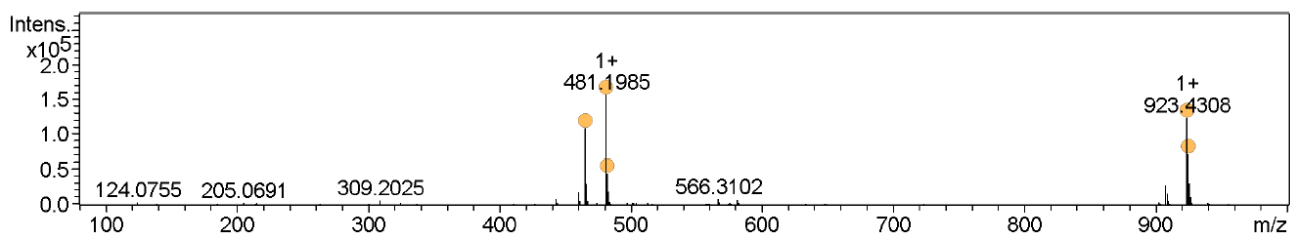
D-sorbitol (1.0 eq.) and 4-toluene sulfonic acid (4-TSA) (0.2 eq.) were transferred into a round-bottomed flask and were stirred in MeOH (100 mL) in room temperature. The aldehyde of choice- cuminaldehyde, vanillin and cinnamaldehyde (1.0 eq. for the mono and 2.0 eq. for the di) was then added dropwise and the reaction was left stirring overnight. The reaction mixture was evaporated under reduced pressure to obtain white solid. The white solid was digested in H<sub>2</sub>O (100 mL) and was filtered under reduced pressure. The filter was then washed with EtOAc (50 mL) followed by Et<sub>2</sub>O (50 mL) and dried in *vacuo* to yield the titled product as a white powder.



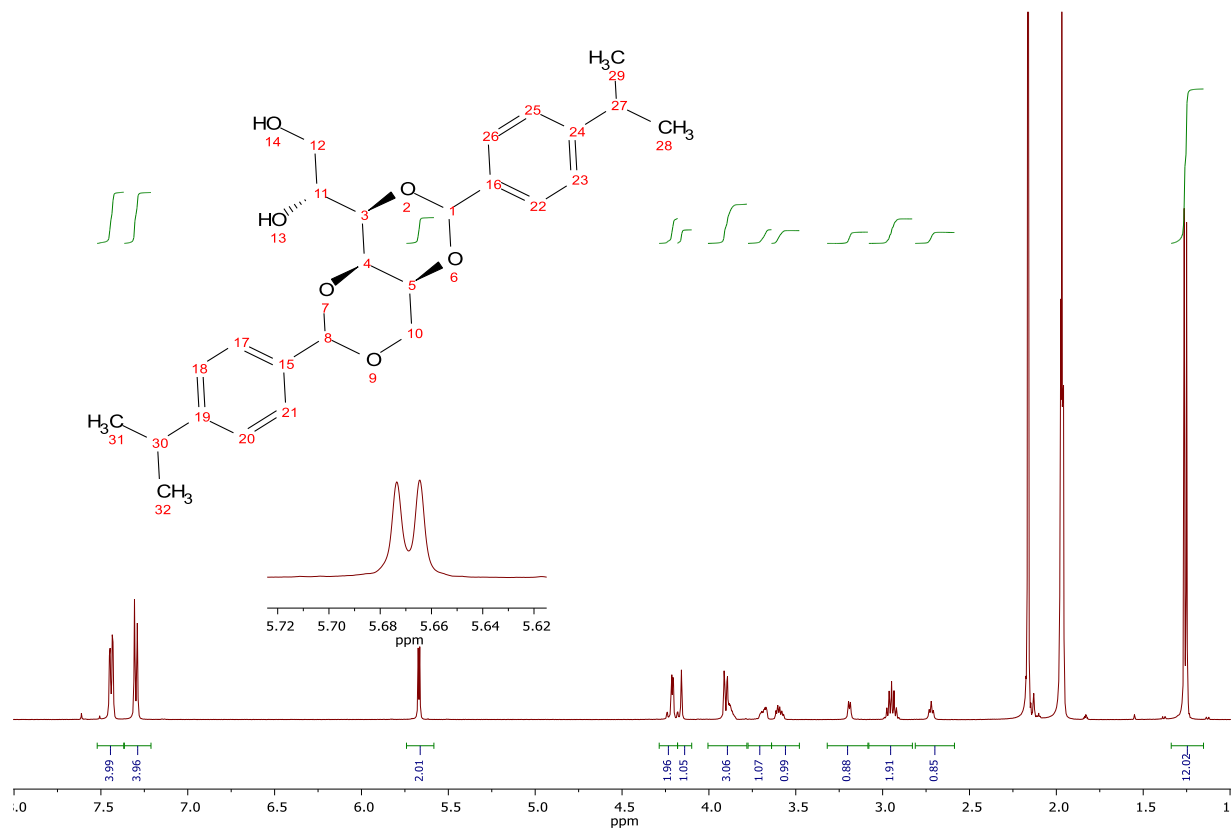
**Synthesis of DBS-*i*Pr:** DBS-*i*Pr: The titled compound was synthesized using the general procedure with cuminaldehyde. Precipitate formed and was filtered instead of evaporation under reduced pressure. Rest of the work-up followed but was further washed with cold MeOH (100 mL) to remove all the MBS-*i*Pr. Yield: (45%). M.p.: 193–195 °C. <sup>1</sup>H NMR (500 MHz, CD<sub>3</sub>CN) δ 7.44 (4H, dd, *J* = 8.4,

2.4, 17-H, 21-H, 26-H, 22-H), 7.30 (4H, d, *J* = 8.0, 18-H, 20-H, 25-H, 23-H), 5.67 (1H, s, 8-H), 5.66 (1H, s, 1-H), 4.21 (2H, dd, *J* = 4.4, 1.8, 10-H<sub>2</sub>), 4.16 (1H, t, *J* = 1.4, 5-H), 3.96 – 3.81 (3H, m, 4-H, 3-H, 11-H), 3.69 (1H, ddd, *J*

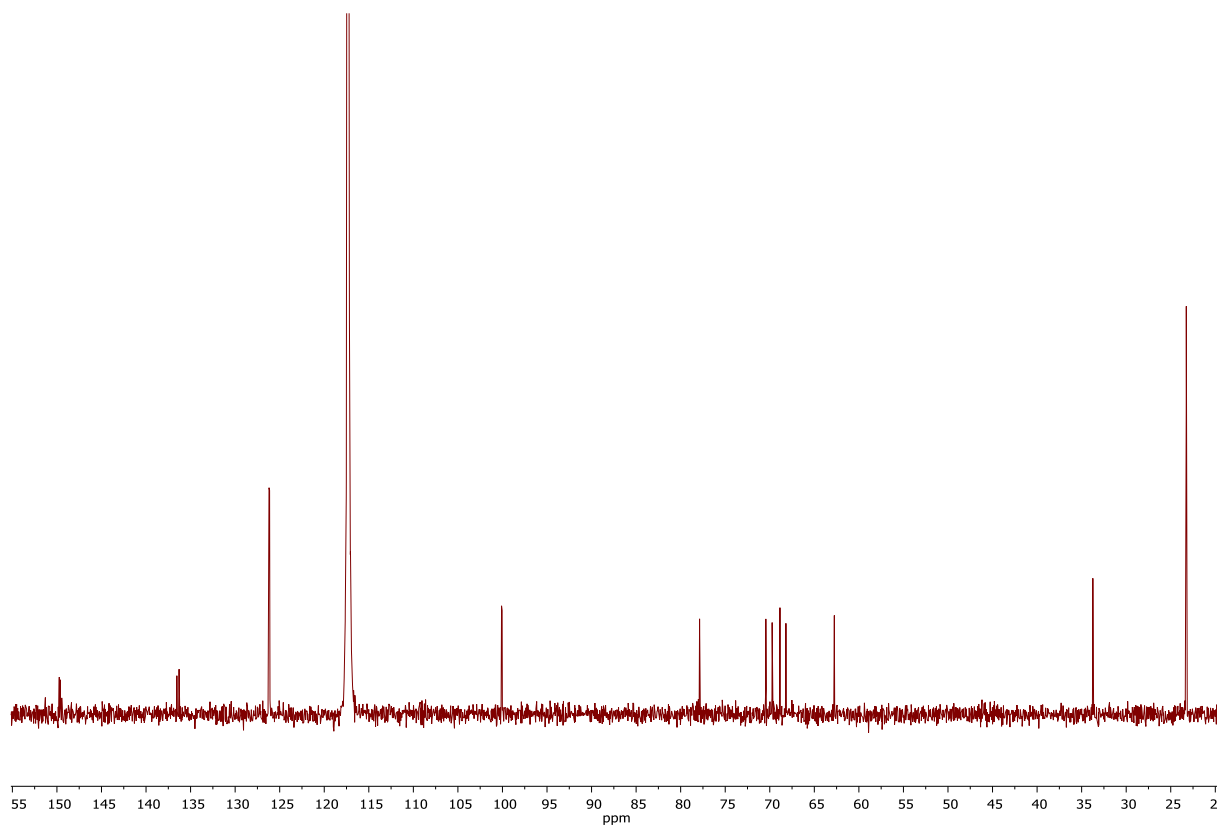
= 11.4, 5.8, 2.7, 12- $H_a$ ), 3.59 (1H, dt,  $J$  = 11.2, 5.3, 12- $H_b$ ), 3.19 (1H, d,  $J$  = 5.4, 13- $H$ ), 2.95 (2H, hept,  $J$  = 6.9, 27- $H$ , 30- $H$ ), 2.72 (1H, t,  $J$  = 6.1, 14- $H$ ), 1.26 (12H, d,  $J$  = 6.9, 28- $H_3$ , 29- $H_3$ , 30- $H_3$ , 31- $H_3$ ).  $^{13}\text{C}$  NMR (101 MHz,  $\text{CD}_3\text{CN}$ )  $\delta$  149.7 (C15), 149.6 (C16), 136.5 (C19), 136.3 (24), 126.2 (C17), 126.2 (C21), 126.1 (C26), 126.1 (C22), 100.1 (C8), 100.0 (C1), 77.9 (C3), 70.4 (C4), 69.7 (C10), 68.9 (C5), 68.2 (C11), 62.8 (C12), 33.7 (C27, C30), 23.3 (C31, C32, C29, C28).  $\nu_{\text{max}}/\text{cm}^{-1}$  3260br (OH sugar), 2954w, 2871w, 1398w, 1339w, 1013s. (ESI)  $m/z$  ( $\text{M}+\text{H}_4\text{N}$ ) $^+$  calcd. for  $\text{C}_{26}\text{H}_{38}\text{NO}_6^+$  460.2694, found 460.2693.  $[\alpha]_D^{25} = +60.0$  (c. 10.0 mg  $\text{mL}^{-1}$ , DMSO). CHN Analysis: Calcd (%) C 70.55; H 7.75; O 21.70; Found (100%) C 68.43, H 7.75, O 23.95.



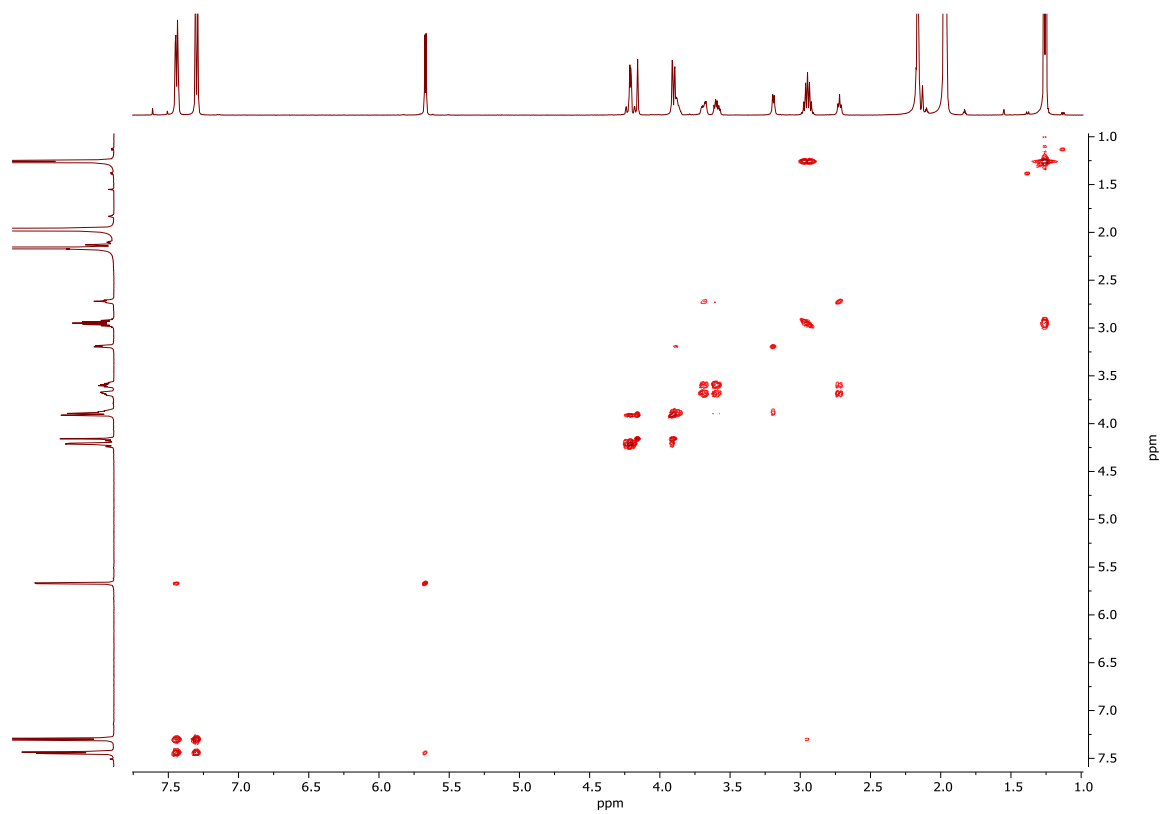
ESI Fig. 1 | HRMS of DBS-*i*Pr in positive mode



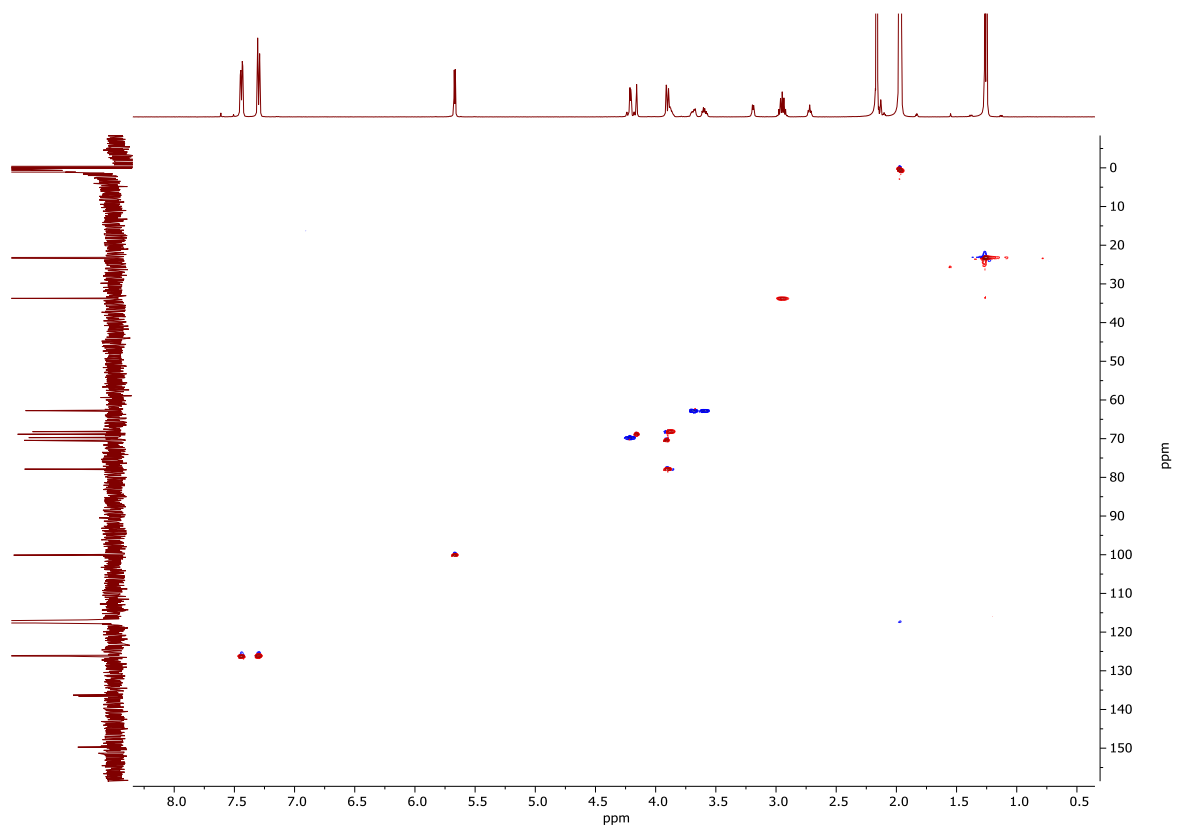
ESI Fig. 2 |  $^1\text{H}$  NMR of DBS-*i*Pr



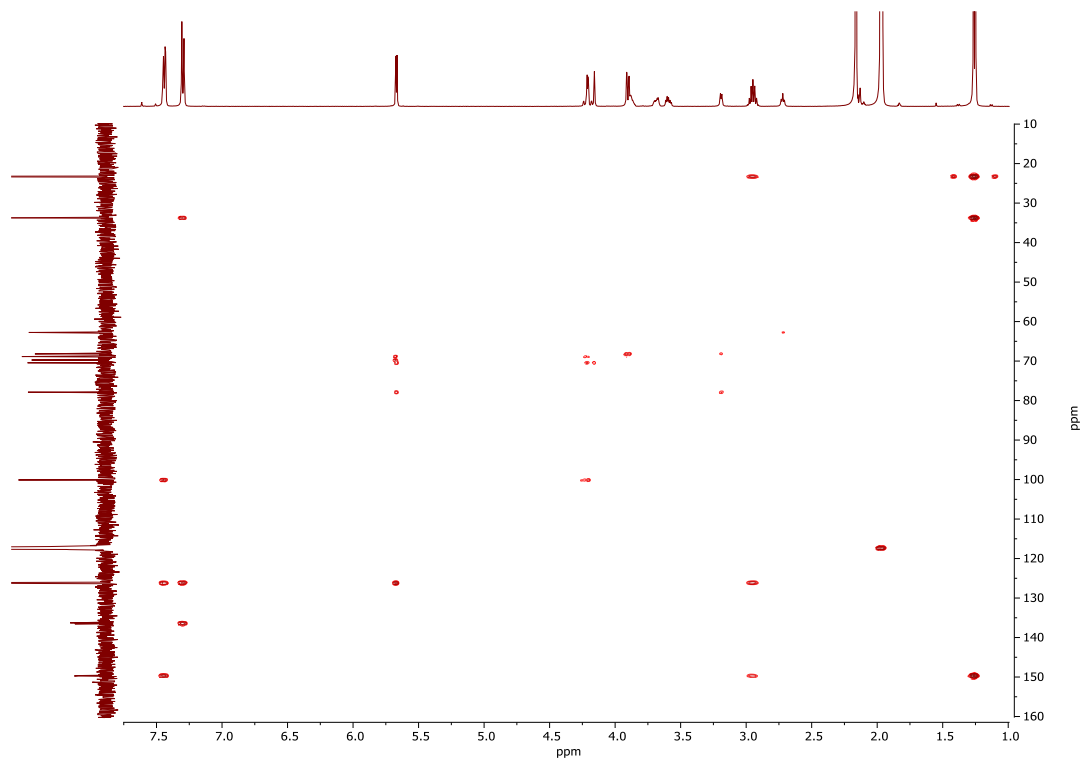
ESI Fig. 3 |  $^{13}\text{C}$  NMR of DBS-*i*Pr



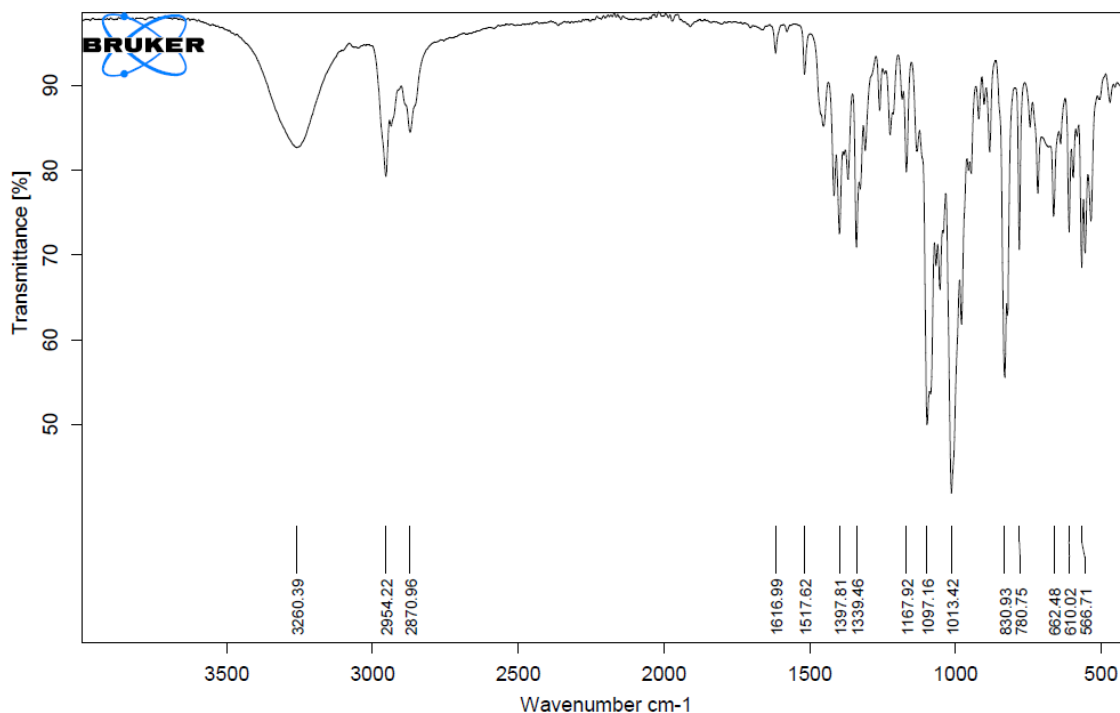
ESI Fig. 4 | COSY of DBS-*i*Pr



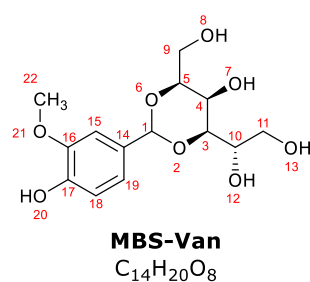
ESI Fig. 5 | HSQC of DBS-iPr



ESI Fig. 6 | HMBC of DBS-iPr



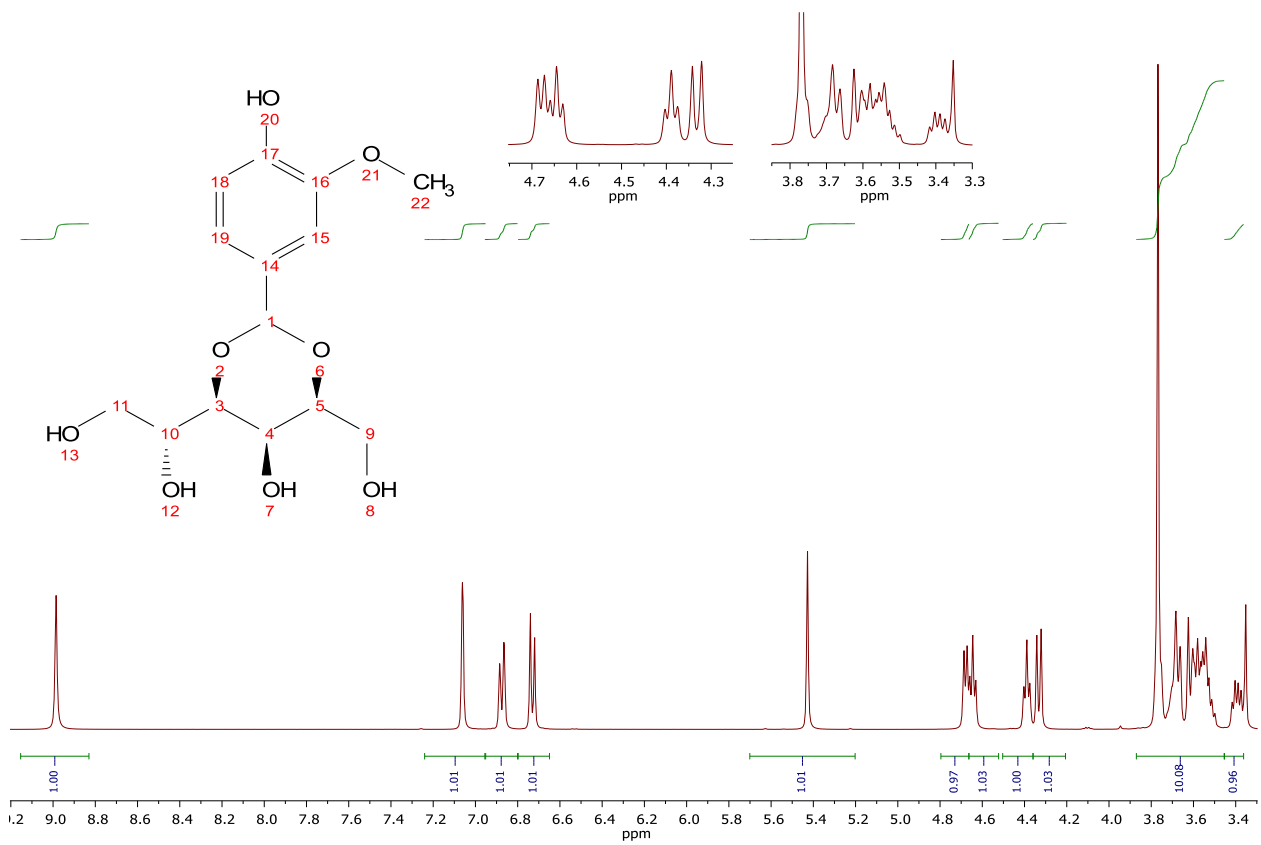
ESI Fig. 7 | IR spectrum of DBS-*i*Pr



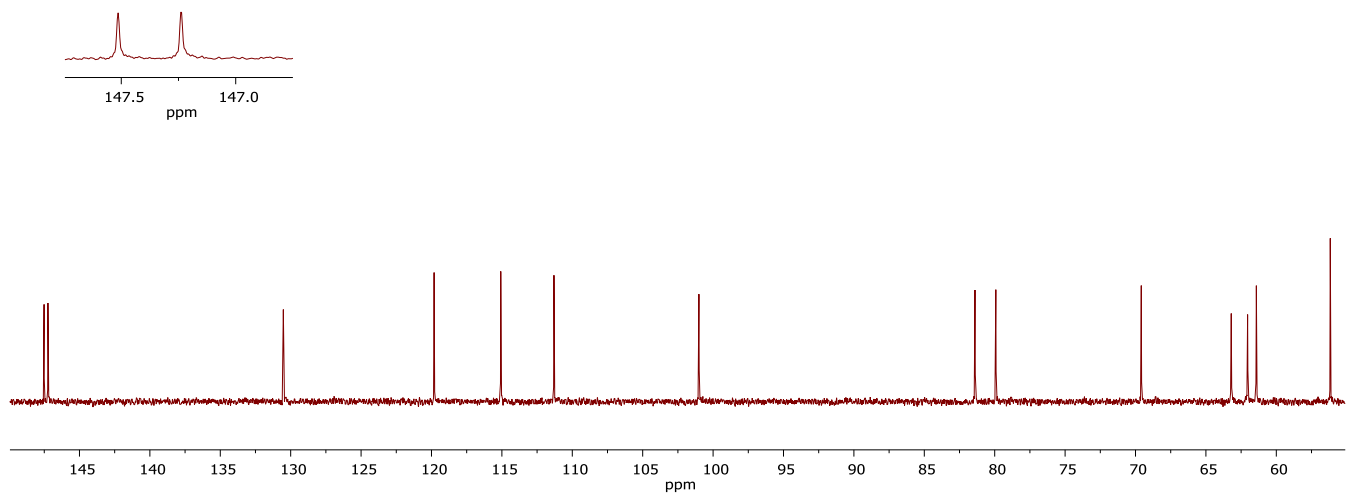
**Synthesis of MBS-Van:** The reaction was carried out in inert atmosphere following

the general procedure. However, this compound was not washed with water because it is soluble in water. Yield (73%). Mp 173 – 175°C. <sup>1</sup>H NMR (400 MHz, DMSO-*d*<sub>6</sub>) δ 8.99 (1H, s, 20-H), 7.06 (1H, s, 15-H), 6.88 (1H, d, *J* = 8.1, 19-H), 6.73 (1H, d, *J* = 8.1, 18-H), 5.43 (1H, s, 1-H), 4.68 (1H, d, *J* = 5.9, 12-H), 4.64 (1H, t, *J* = 5.8, 8-H), 4.39 (1H, t, *J* = 5.8, 13-H), 4.33 (1H, d, *J* = 8.2, 7-H), 3.77 – 3.73 (4H, m, 22-H<sub>3</sub>, 5-H), 3.73 – 3.65 (2H, m, 10-H, 4-H), 3.64 – 3.49 (4H, m, 3-H, 9-H<sub>2</sub>, 11-H<sub>b</sub>), 3.42 – 3.37 (1H, m, 11-H<sub>a</sub>).

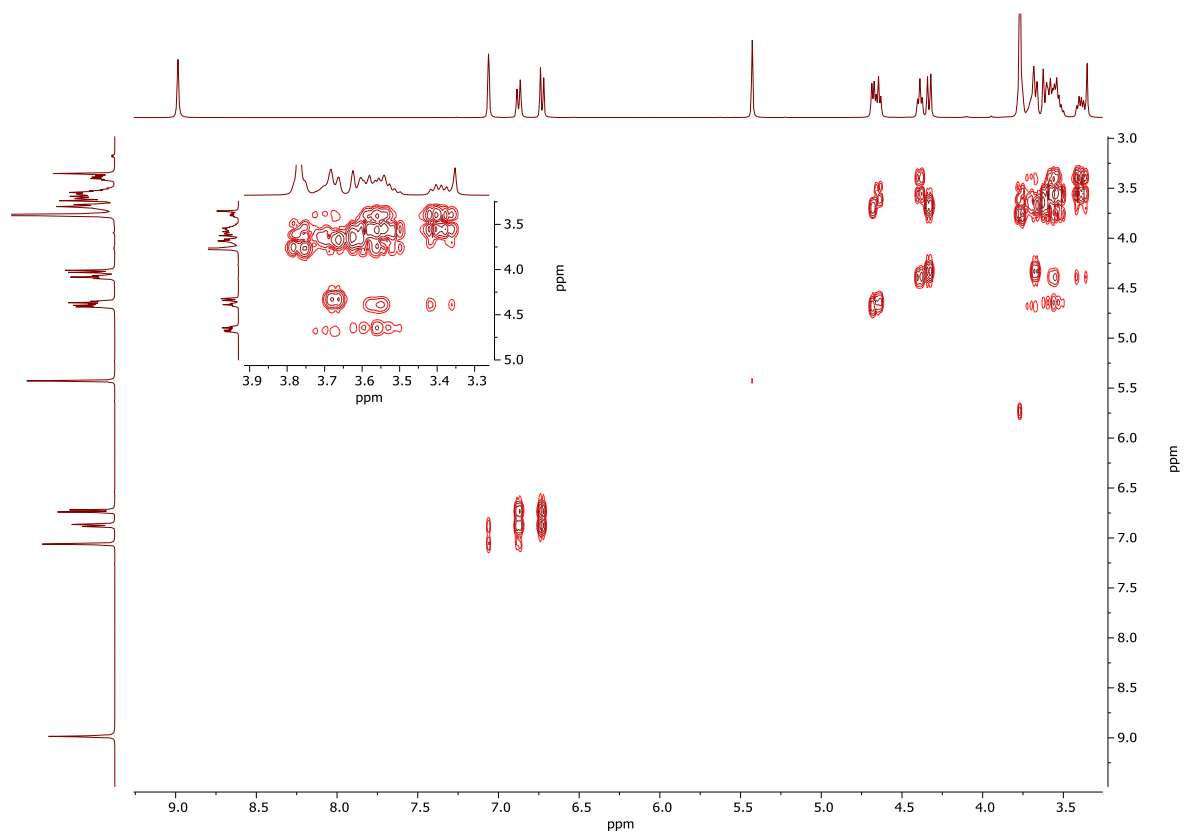
<sup>13</sup>C NMR (100 MHz, DMSO-*d*<sub>6</sub>) δ 147.5 (C17), 147.2 (C14), 130.5 (C16), 119.8 (C19), 115.1 (C18), 111.3 (C15), 101.0 (C1), 81.4 (C5), 79.9 (C3), 69.6 (C10), 63.2 (C11), 62.1 (C4), 61.4 (C9), 56.2 (C22). *v*<sub>max</sub>/cm<sup>-1</sup> 3461w (Ph-OH), 3262br (OH sugar), 2967w, 1618w, 1095s, 1016s. (ESI) *m/z* (M+Na)<sup>+</sup> calcd. for C<sub>14</sub>H<sub>20</sub>NaO<sub>8</sub><sup>+</sup> 339.1050, found 339.1043. [α]<sup>25</sup><sub>D</sub> = + 8.00 (c. 10.0 mg mL<sup>-1</sup>, H<sub>2</sub>O). CHN Analysis: Calcd (%) C 54.86; H 6.14; O 39.00; Found (100%) C 53.12, H 6.44, O 40.44.



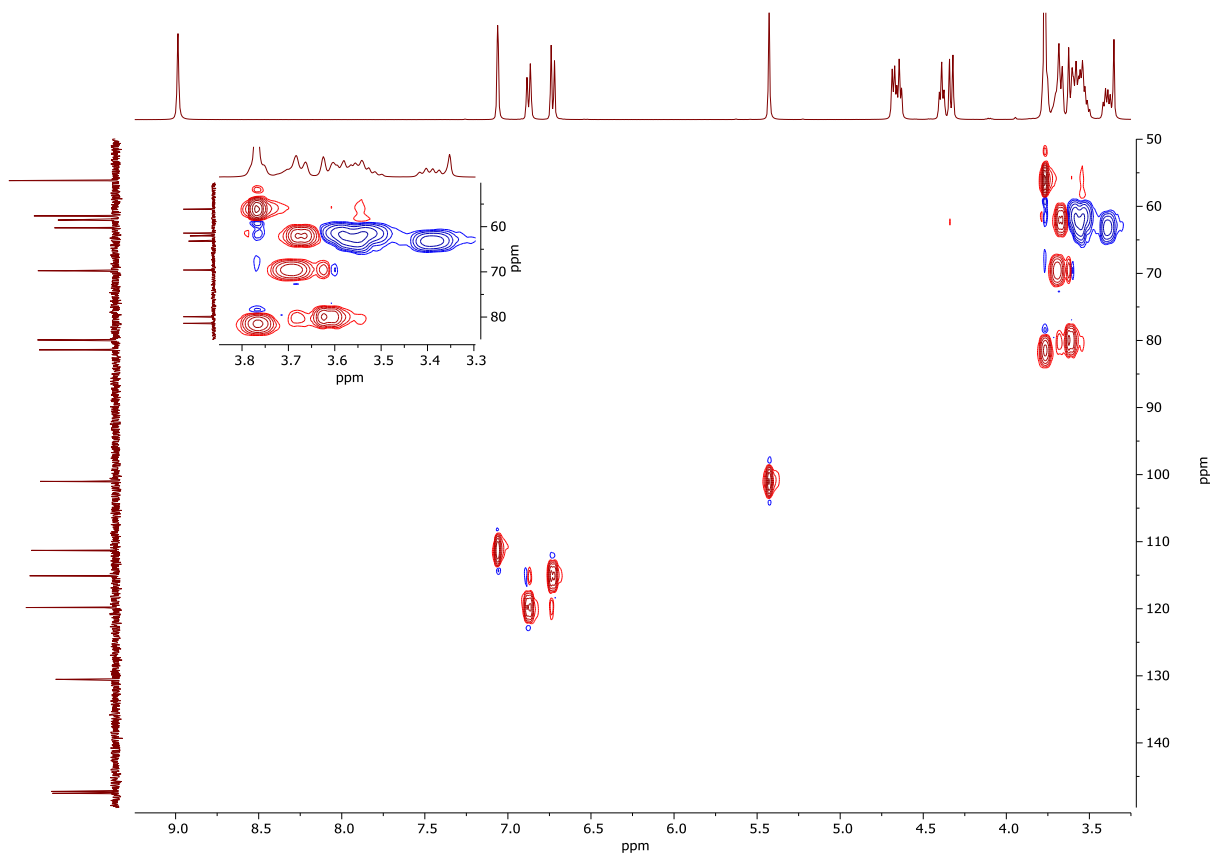
ESI Fig. 8 | <sup>1</sup>H NMR of MBS-Van



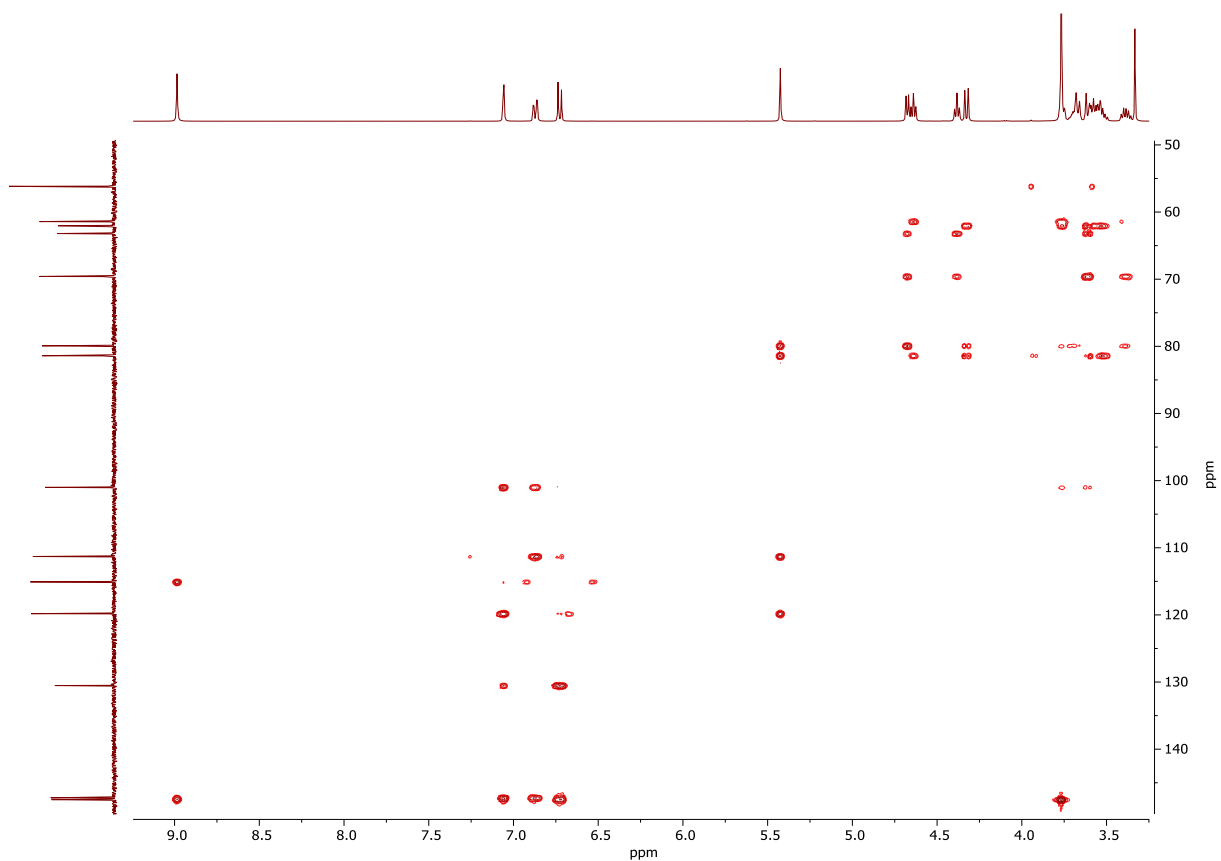
ESI Fig. 9 | <sup>13</sup>C NMR of MBS-Van



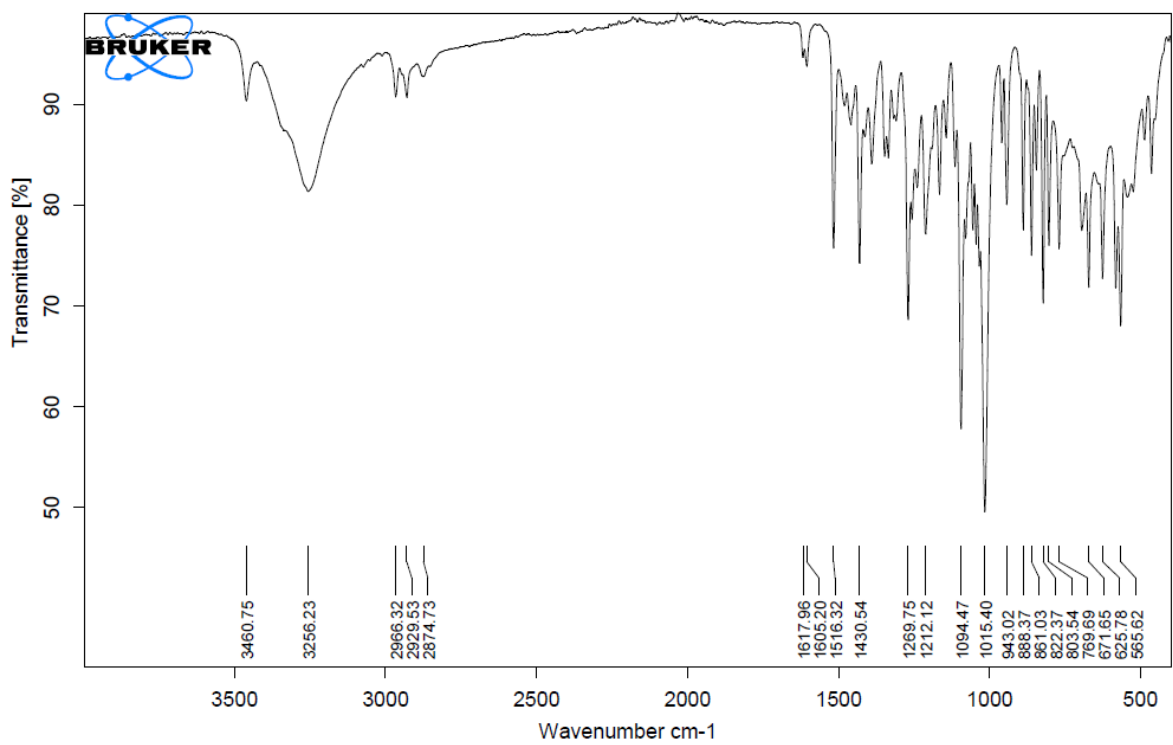
ESI Fig. 10 | COSY of MBS-Van



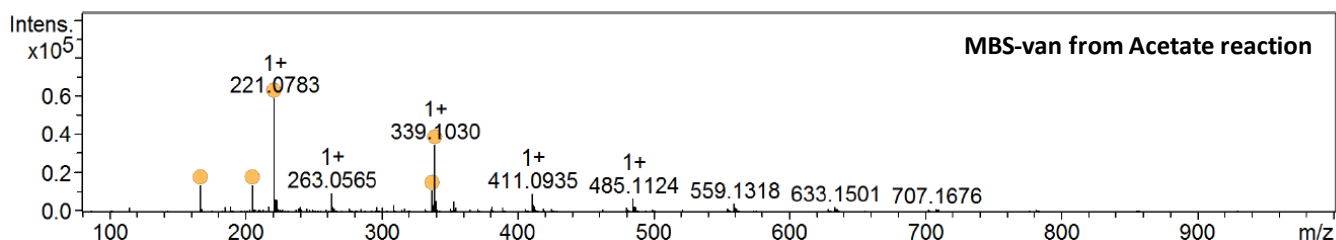
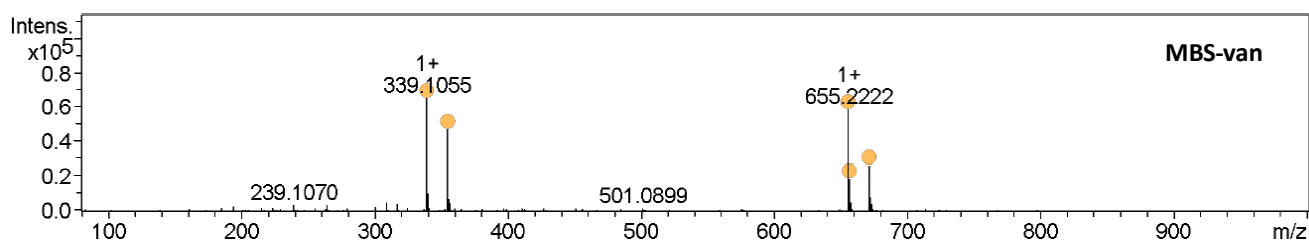
ESI Fig. 11 | HSQC of MBS-Van



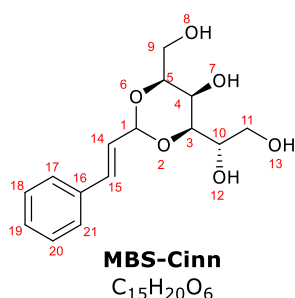
ESI Fig. 12 | HMBC of MBS-Van



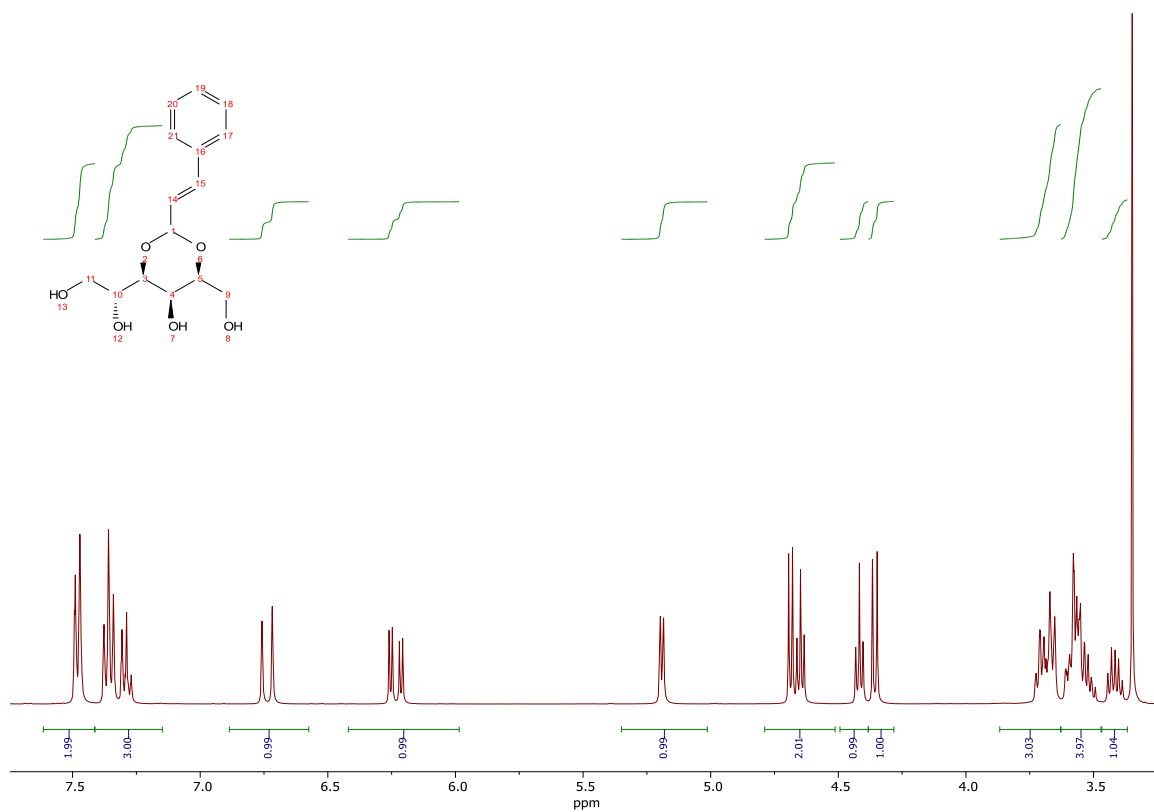
ESI Fig. 13 | IR spectrum of MBS-Van



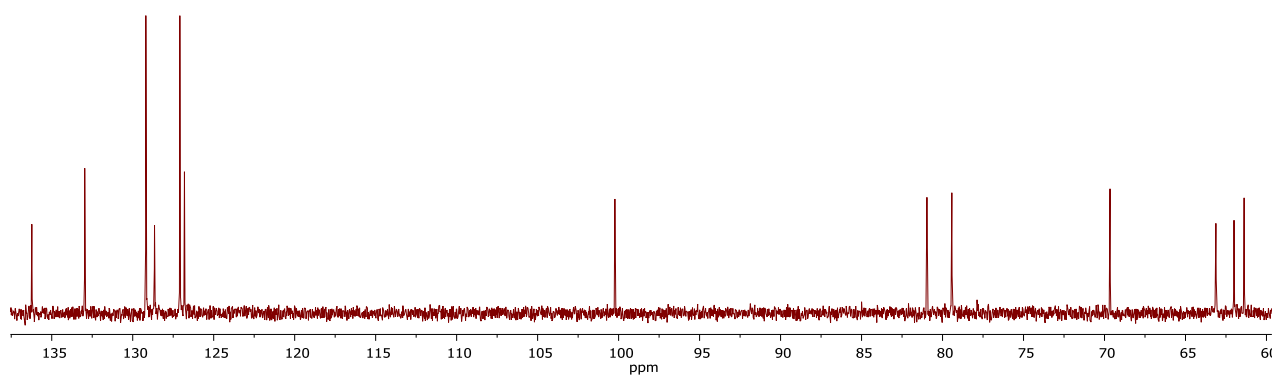
ESI Fig. 14 | HRMS of MBS-Van



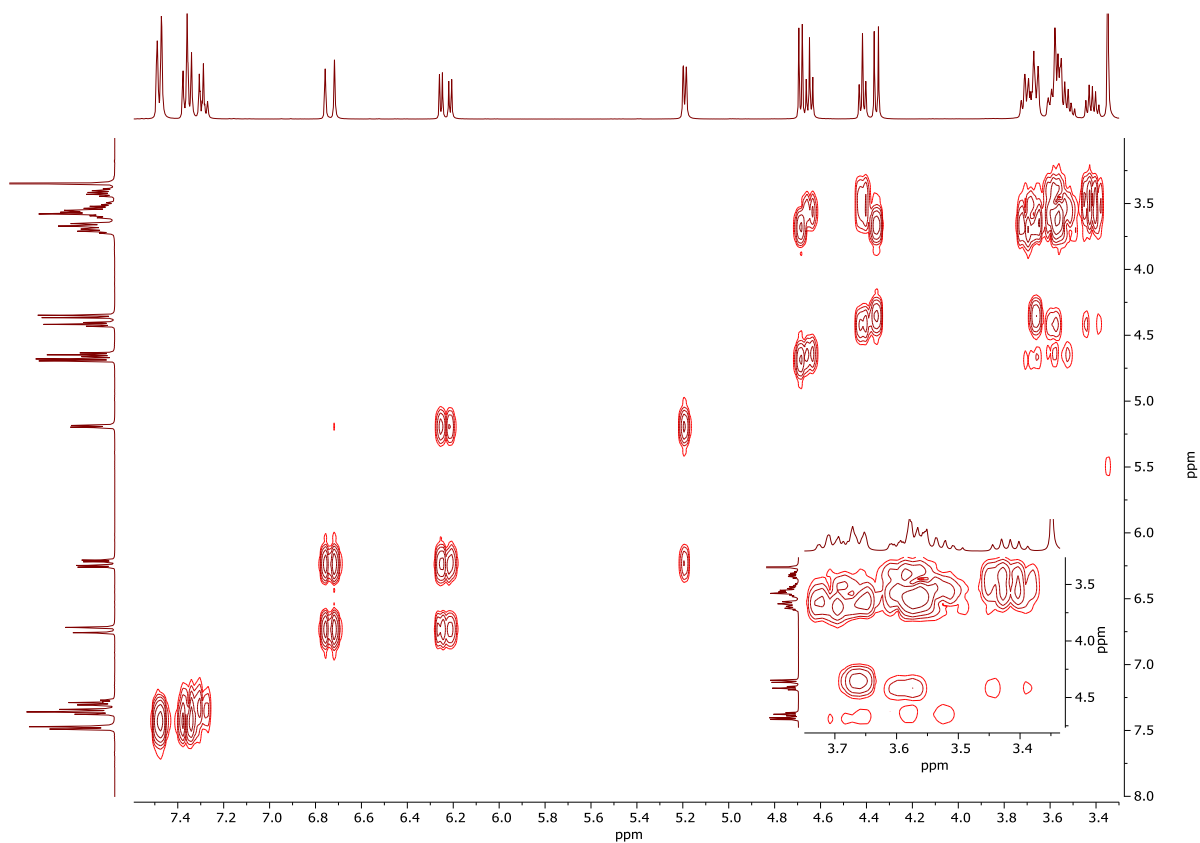
**Synthesis of MBS-Cinn:** The titled compound was synthesized via general procedure. Yield a white solid (68%). Mp 124 – 126 °C. <sup>1</sup>H NMR (400 MHz, DMSO-*d*<sub>6</sub>) δ 7.51 – 7.46 (2H, m, 17-*H*, 21-*H*), 7.40 – 7.33 (2H, m, 18-*H*, 20-*H*), 7.32 – 7.26 (1H, m, 19-*H*), 6.74 (1H, d, *J* = 16.2, 14-*H*), 6.23 (1H, dd, *J* = 16.2, 5.1, 15-*H*), 5.19 (1H, dd, *J* = 5.1, 1.1, 1-*H*), 4.69 (1H, d, *J* = 6.0, 12-*H*), 4.65 (1H, t, *J* = 5.7, 8-*H*), 4.42 (1H, t, *J* = 5.8, 13-*H*), 4.36 (1H, d, *J* = 7.3, 7-*H*), 3.74 – 3.64 (3H, m, 5-*H*, 10-*H*, 4-*H*), 3.62 – 3.48 (4H, m, 3-*H*, 9-*H*<sub>2</sub>, 11-*H*<sub>b</sub>), 3.42 (1H, dt, *J* = 11.3, 5.7, 11-*H*<sub>a</sub>) ppm. <sup>13</sup>C NMR (100 MHz, DMSO-*d*<sub>6</sub>) δ 136.2 (C16), 133.0 (C14), 129.2 (C17, C21), 128.7 (C19), 127.1 (C18, C20), 126.8 (C15), 100.2 (C1), 81.0 (C5), 79.4 (C3), 69.7 (C10), 63.1 (C11), 62.0 (C4), 61.4 (C9) ppm.  $\nu_{\max}/\text{cm}^{-1}$  3271br (OH sugar), 2933w, 2864w, 965s. (ESI) *m/z* (M+Na)<sup>+</sup> calcd. for C<sub>15</sub>H<sub>20</sub>NaO<sub>6</sub><sup>+</sup> 319.1152, found 319.1144.  $[\alpha]_{\text{D}}^{25} = + 8.00$  (c. 10.0 mg mL<sup>-1</sup>, MeOH). CHN Analysis: Calcd (%) C 60.78; H 6.81; O 32.41; Found (100%) C 58.00, H 6.69, O 35.31.



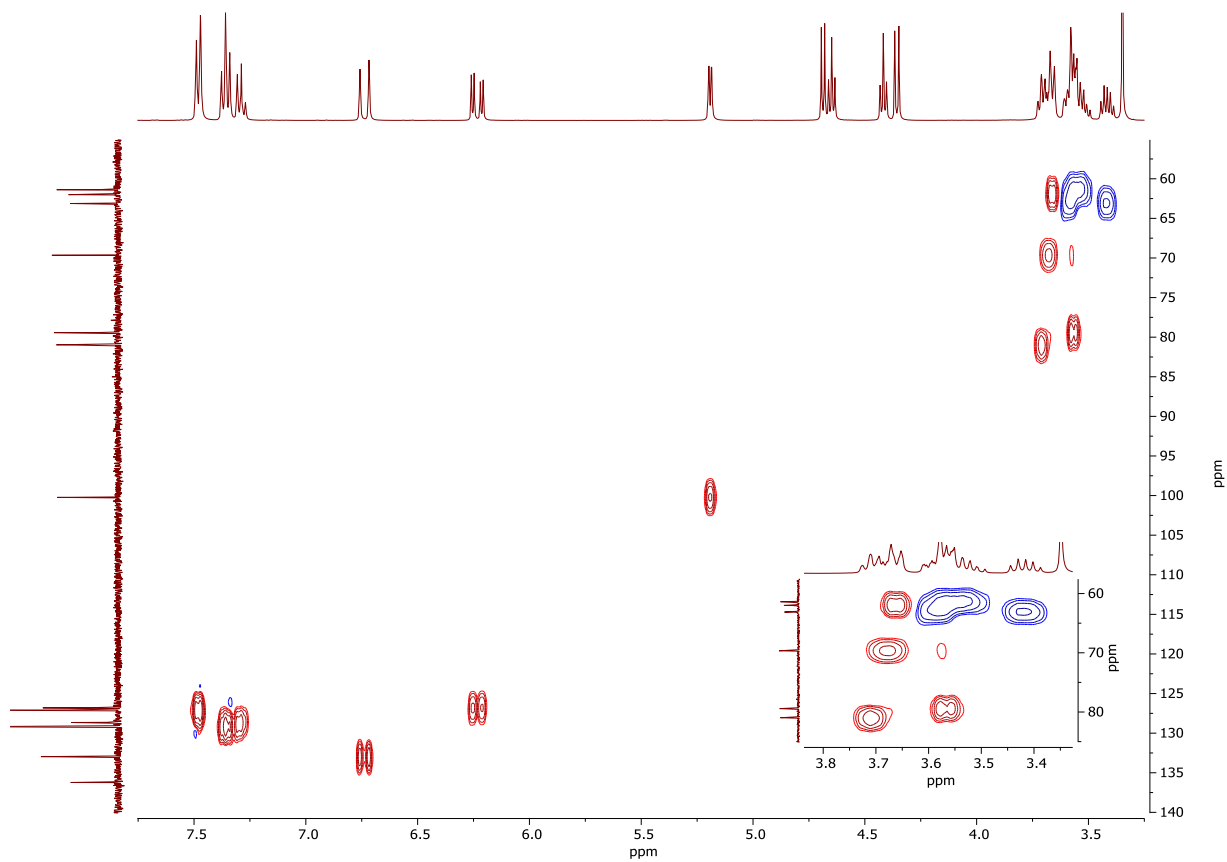
ESI Fig. 15 | <sup>1</sup>H NMR of MBS-Cinn



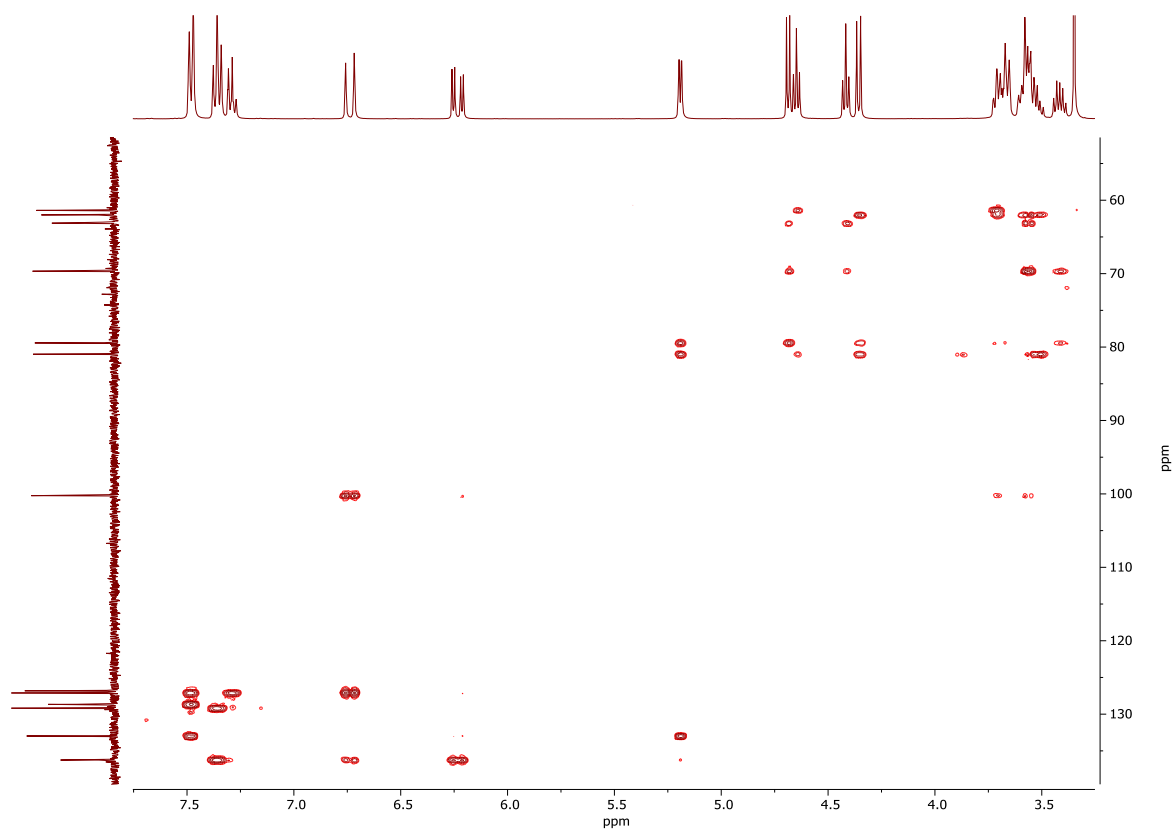
ESI Fig. 16 | <sup>13</sup>C NMR of MBS-Cinn



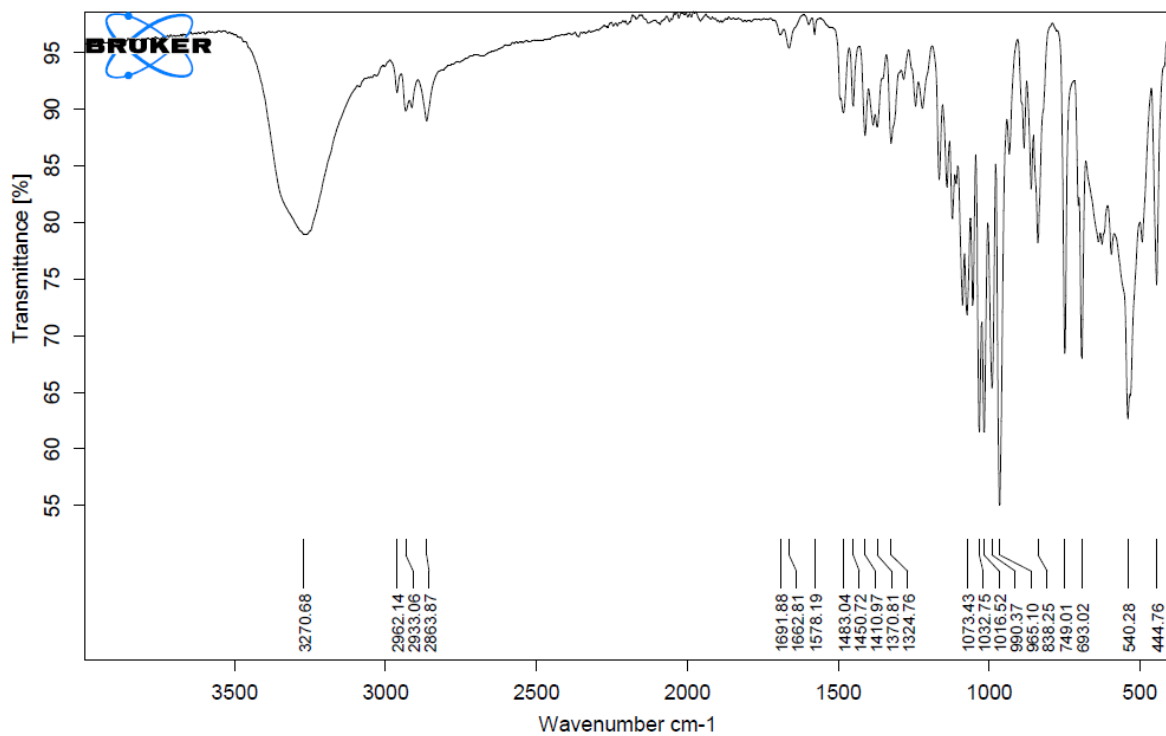
ESI Fig. 17 | COSY of MBS-Cinn



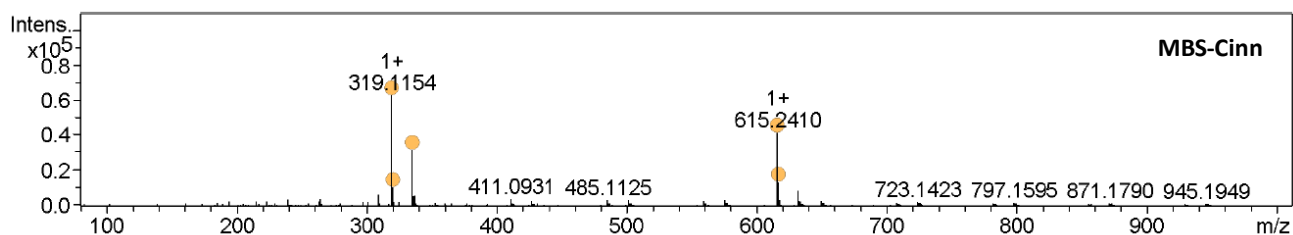
ESI Fig. 18 | HSQC of MBS-Cinn



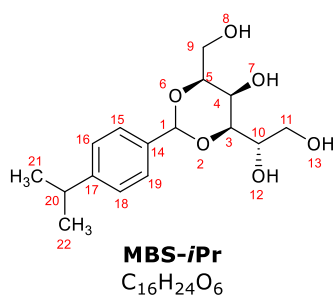
ESI Fig. 19 | HMBC of MBS-Cin



ESI Fig. 20 | IR Spectrum of MBS-Cinn

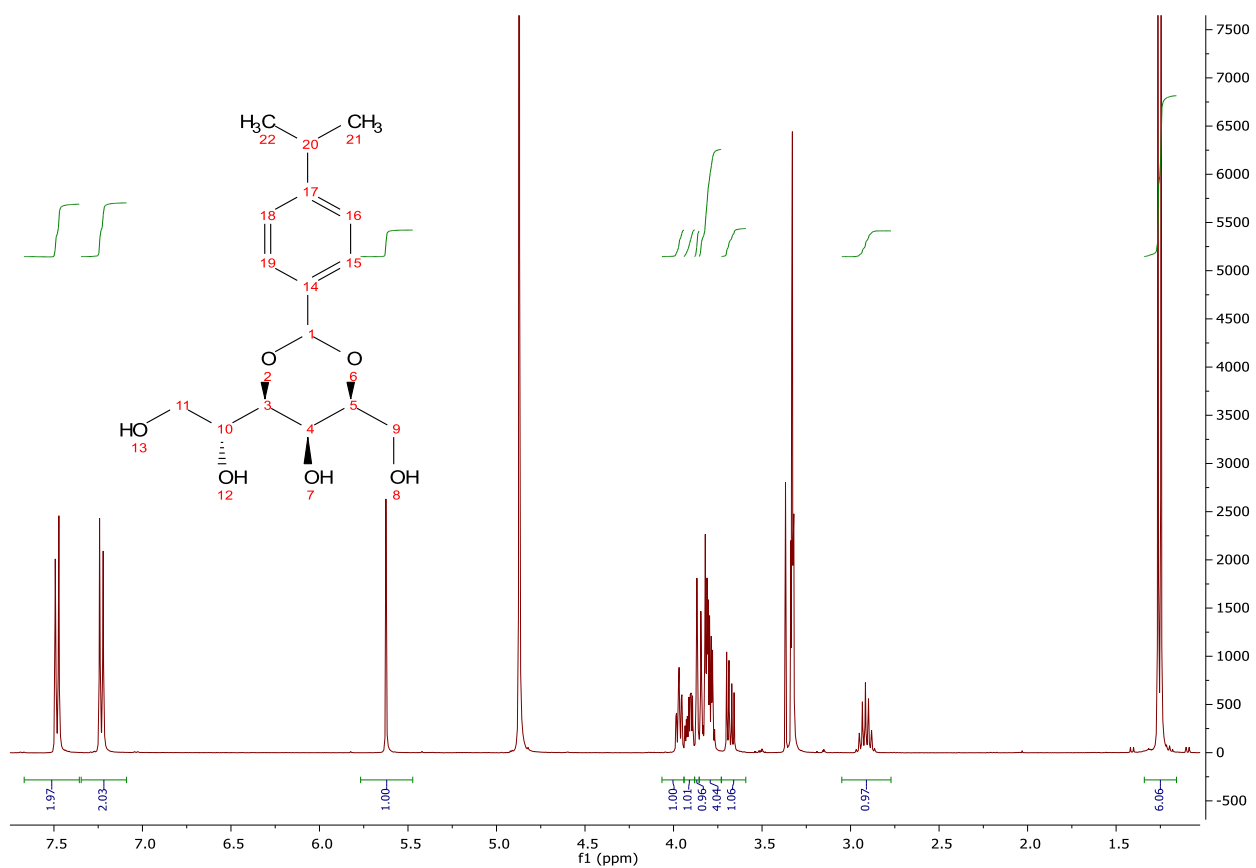


ESI Fig. 21 | HRMS of MBS-Cinn

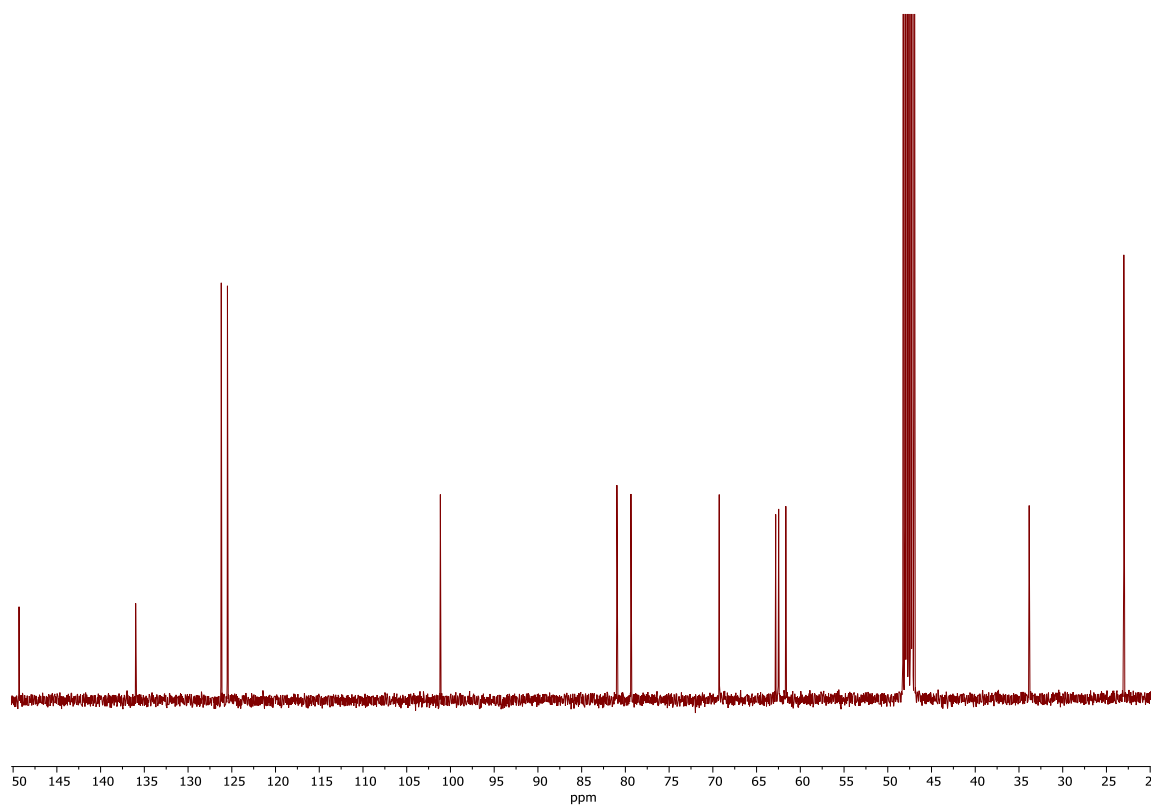


**Synthesis of MBS-iPr:** The titled compound was synthesized via general procedure to yield a white solid. Yield (59%). Mp 131 – 133 °C. <sup>1</sup>H NMR (400 MHz, CD<sub>3</sub>OD) δ 7.48 (2H, d, *J* = 8.1, 15-H, 19-H), 7.23 (2H, d, *J* = 8.1, 16-H, 18-H), 5.62 (1H, s, 1-H), 3.97 (1H, ddd, *J* = 6.4, 5.7, 1.4, 5-H), 3.91 (1H, ddd, 8.8, 5.1, 2.9, 10-H), 3.87 (1H, t, *J* = 1.4, 4-H), 3.85 – 3.83 (1H, m, 3-H), 3.83 – 3.76 (3H, m, 9-H<sub>2</sub>, 11-H<sub>b</sub>), 3.68 (1H, dd, *J* = 11.5, 5.2, 11-H<sub>a</sub>), 2.92 (1H, hept, *J* = 6.9, 20-H),

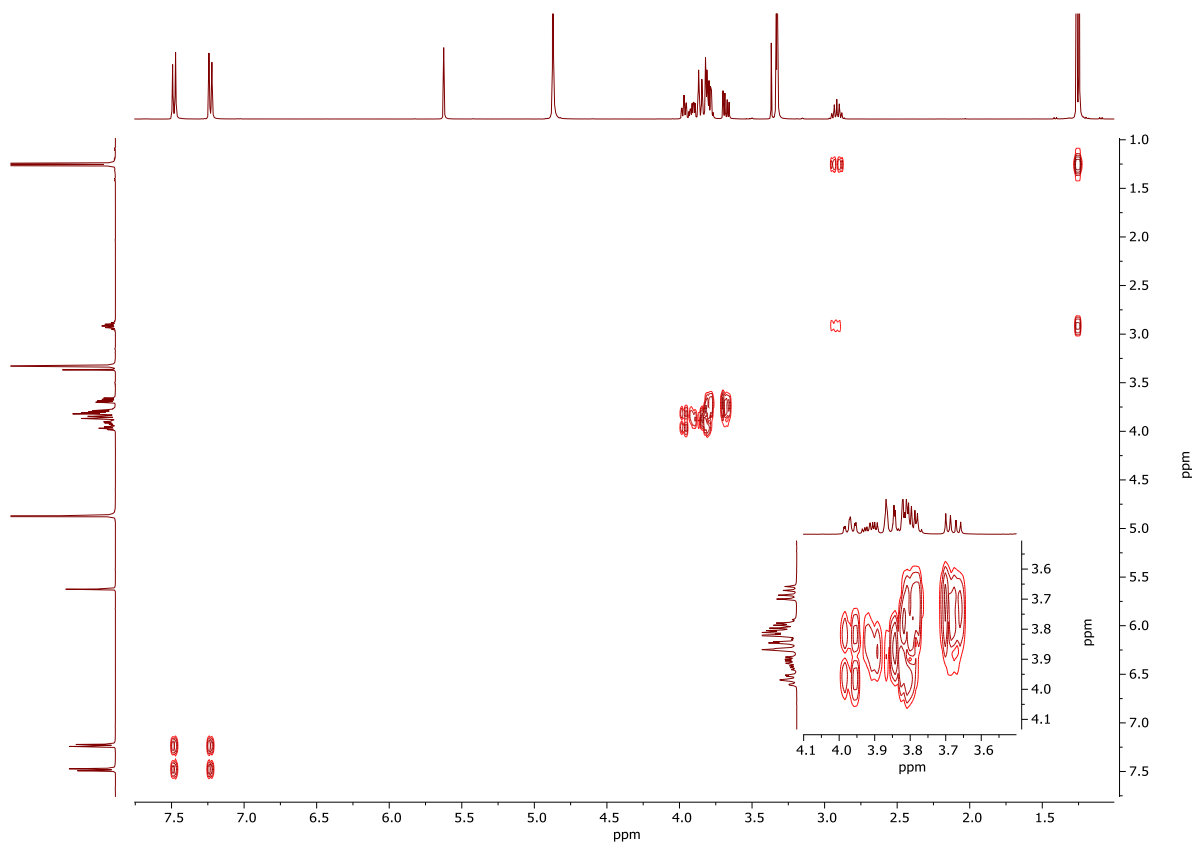
1.25 (6H, d, *J* = 6.9, 21-H<sub>3</sub>, 22-H<sub>3</sub>). <sup>13</sup>C NMR (100 MHz, CD<sub>3</sub>OD) δ 149.3 (C14), 136.0 (C17), 126.2 (C19, C15), 125.5 (C18, C16), 101.2 (C1), 81.0 (C5), 79.4 (C3), 69.3 (C10), 62.8 (C11), 62.5 (C4), 61.7 (C9), 33.8 (C20), 23.0 (C21, C22).  $\nu_{\max}/\text{cm}^{-1}$  3282br (OH sugar), 2941w, 2868w, 1402w, 1098s, 1017s. (ESI) *m/z* (M+Na)<sup>+</sup> calcd. for C<sub>16</sub>H<sub>24</sub>NaO<sub>6</sub><sup>+</sup> 355.1465, found 335.1454.  $[\alpha]^{25}_{\text{D}} = +41.0$  (c. 10.0 mg mL<sup>-1</sup>, MeOH). CHN Analysis: Calcd (%) C 61.51; H 7.75; O 30.74; Found (100%) C 61.51, H 7.79, O 30.70.



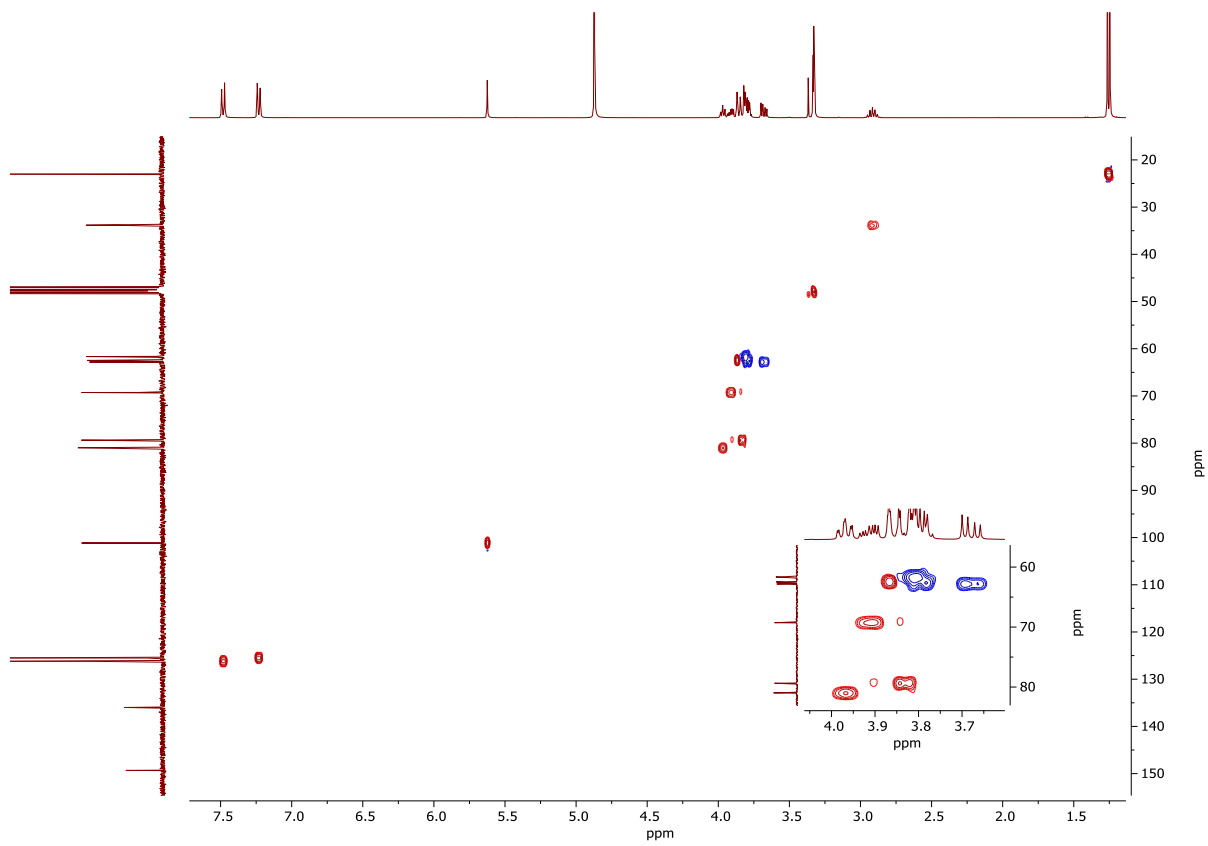
ESI Fig. 22 | <sup>1</sup>H NMR of MBS-iPr



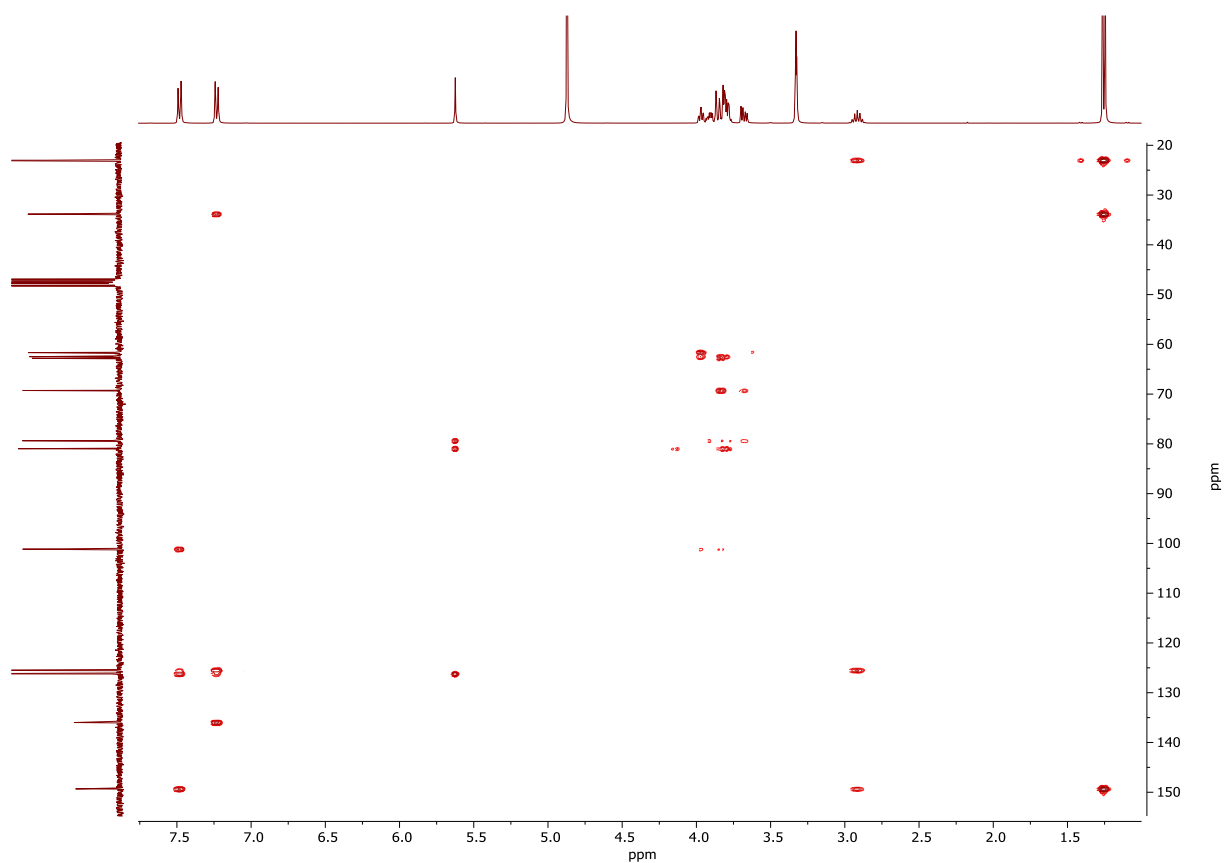
ESI Fig. 23 | <sup>13</sup>C NMR of MBS-iPr



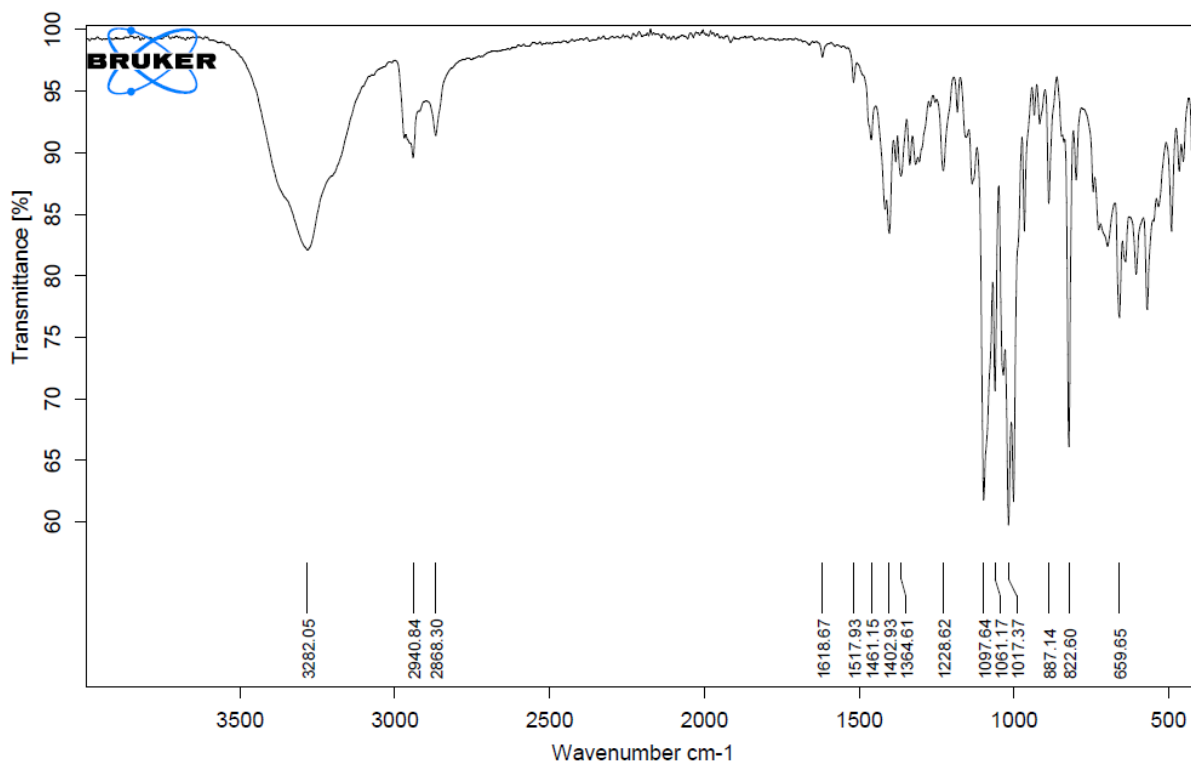
ESI Fig. 24 | COSY of MBS-iPr



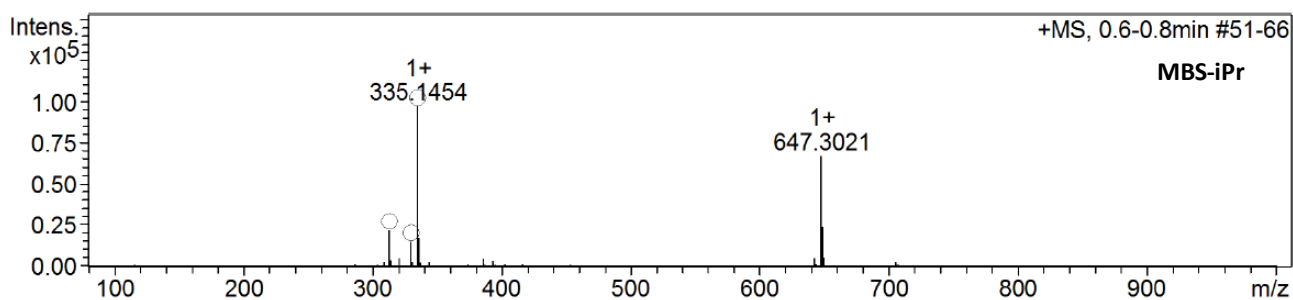
ESI Fig. 25 | HSQC of MBS-iPr



ESI Fig. 26 | HMBC of MBS-iPr



ESI Fig. 27 | IR spectrum of MBS-iPr



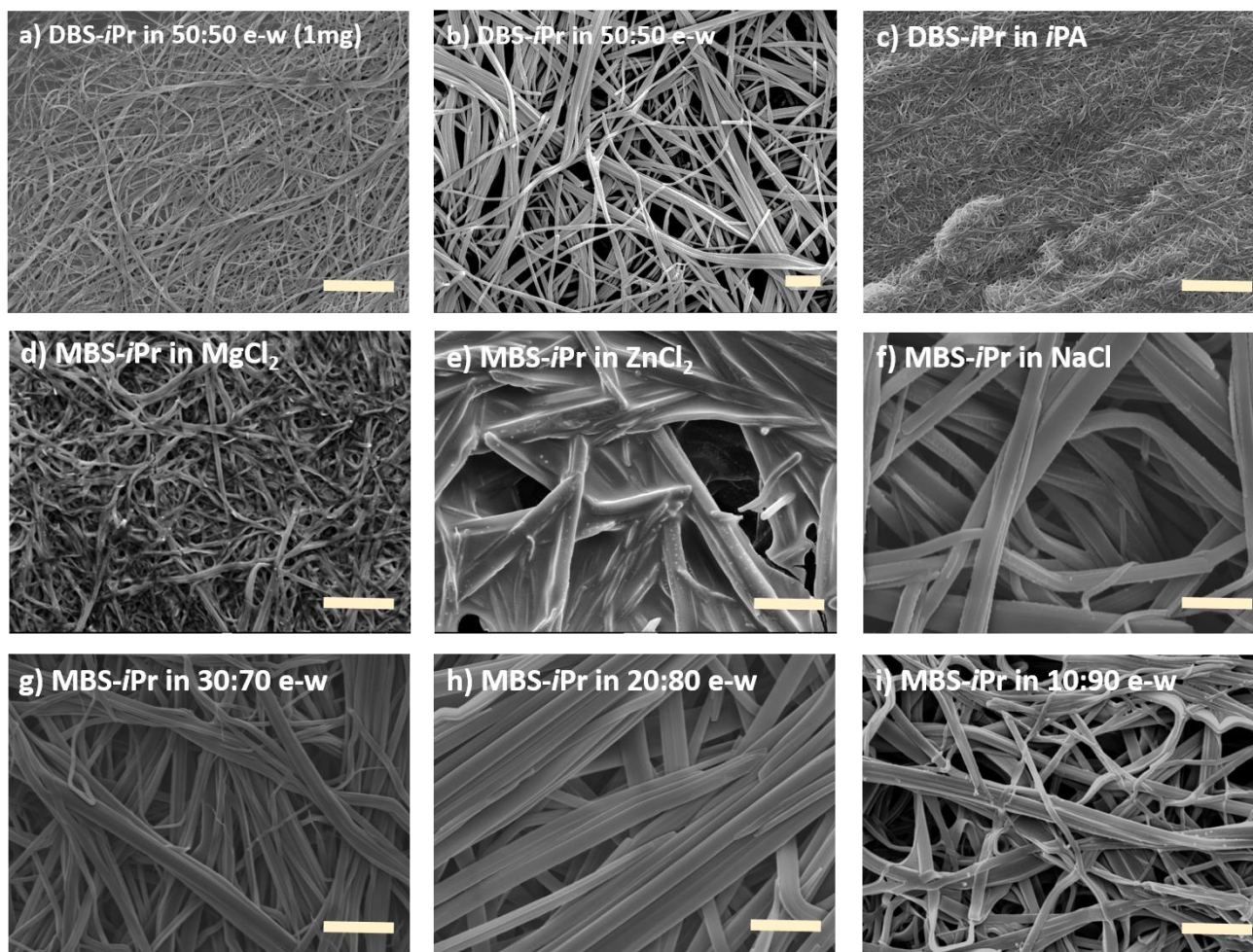
ESI Fig. 28 | HRMS of MBS-iPr

Ethanol:Water Volume Ratio	EtOH	S	P	P	G (O)	G (O)	G (O)
	90:10	S	P	P	G (O)	G (O)	G (O)
	80:20	S	P	G (O)	G (O)	G (O)	G (O)
	70:30	PG (T)	G (O)	G (O)	G (O)	G (O)	G (O)
	60:40	G (T)	G (O)	G (O)	G (O)	G (O)	G (O)
	50:50	G (T)	G (O)	G (O)	G (O)	G (O)	G (O)
	40:60	G (T)	G (O)	G (O)	G (O)	G (O)	G (O)
	30:70	G (T) <sup>b</sup>	G (O)	G (O)	G (O)	G (O) <sup>a</sup>	G (O) <sup>a</sup>
	20:80	G (T) <sup>b</sup>	G (O)	G (O)	G (O) <sup>a</sup>	G (O) <sup>a</sup>	G (O) <sup>a</sup>
	10:90	PG (T) <sup>a</sup>	G (T) <sup>a</sup>	G (O)	G (O) <sup>a</sup>	G (O) <sup>a</sup>	G (O) <sup>a</sup>
	H <sub>2</sub> O	I	I	I	I	I	I
		1	3	5	7	10	15
Concentration of DBS-iPr (mg/mL)							

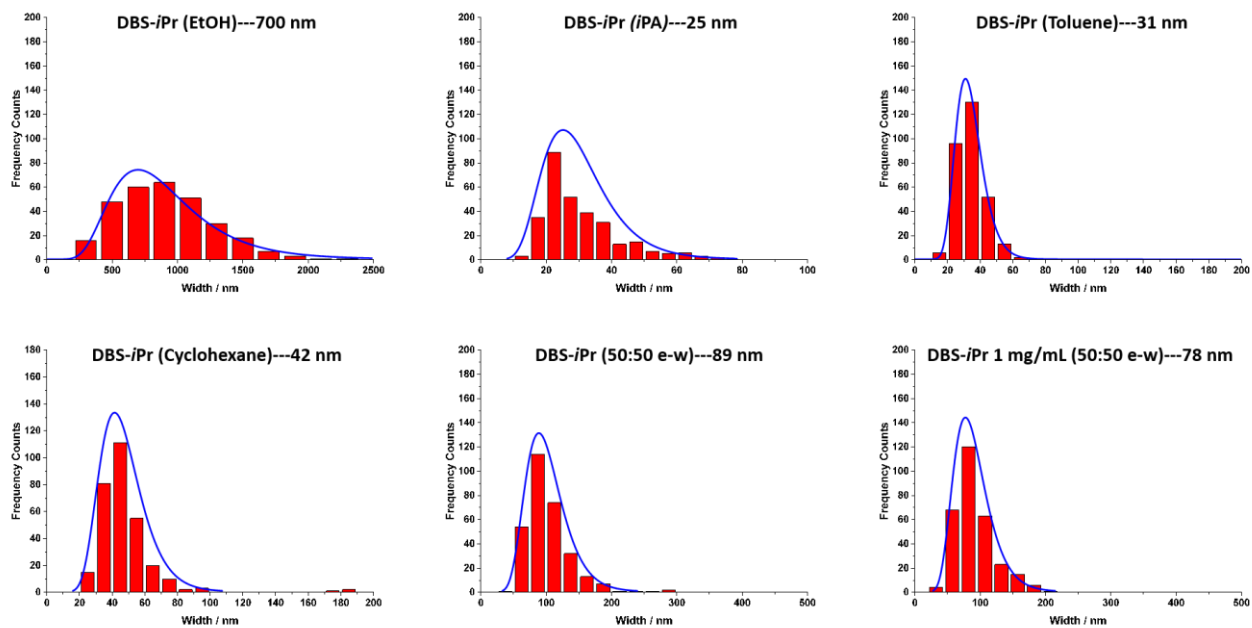
Ethanol:Water Volume Ratio	50:50	S	S	S	S	S	S	P
	40:60	S	S	S	S	P	P	G (O) <sup>b</sup>
	30:70	S	S	P	G (O)	G (O)	G (O)	G (O)
	20:80	S	S	P	G (O)	G (O)	G (O)	G (O)
	10:90	S	S	P	G (O)	G (O)	G (O)	G (O)
	H <sub>2</sub> O	S	PG (O)	G (O)				
		3	5	7	10	15	20	25
Concentration of MBS-iPr (mg/mL)								

ESI Fig. 29 | DBS-iPr and MBS-iPr phase diagram. I = insoluble, G = gel, S = solution, P = precipitate, PG = Partial Gel (PG), (T) = transparent, (O) = opaque. <sup>b</sup>gelation occurred overnight

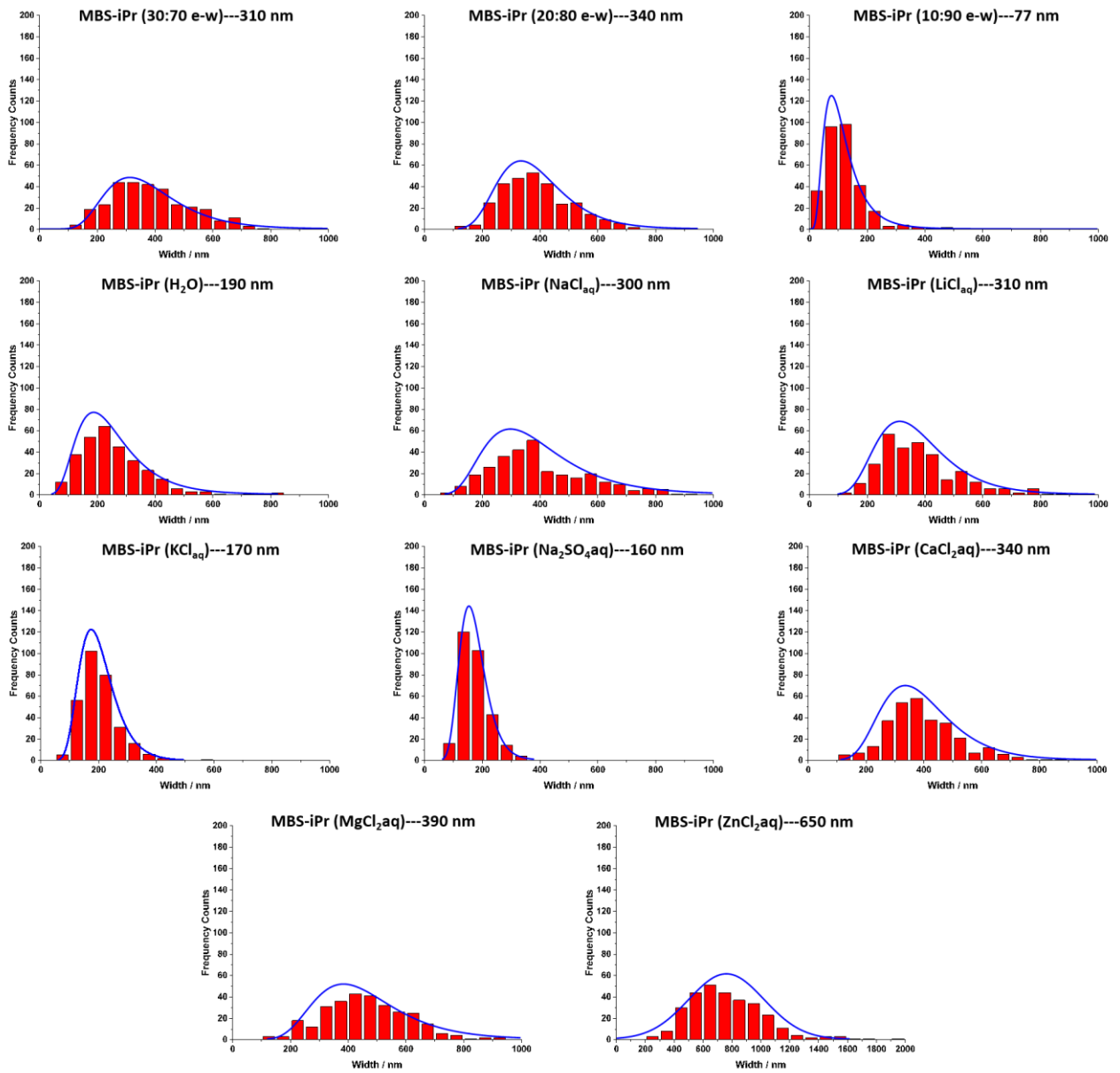
## Morphologies



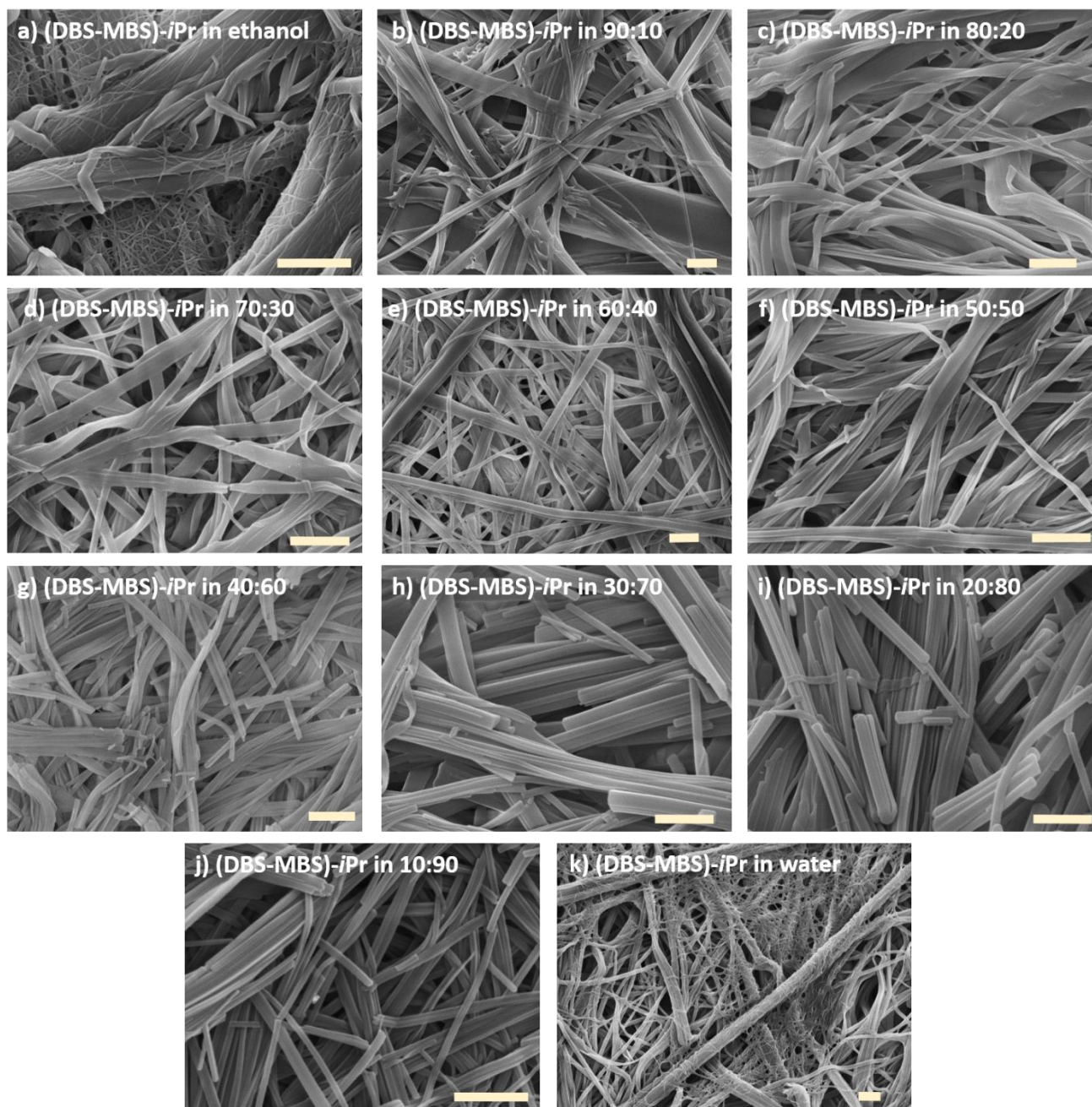
ESI Fig. 30 | SEM micrographs of DBS-*i*Pr and MBS-*i*Pr xerogels formed in different solvents. All in 1% w/v (except a – 0.1% w/v) upon heating and cooling. Conditions: xerogel prepared by drying the gel in air and then coating with 5nm IR before imaging under vacuum at 5kV. Scale bar in all images is 1 μm.



ESI Fig. 31 | Distribution histograms for DBS-iPr xerogels width fibre dimensions from SEM images all at 10 mg/mL unless stated.

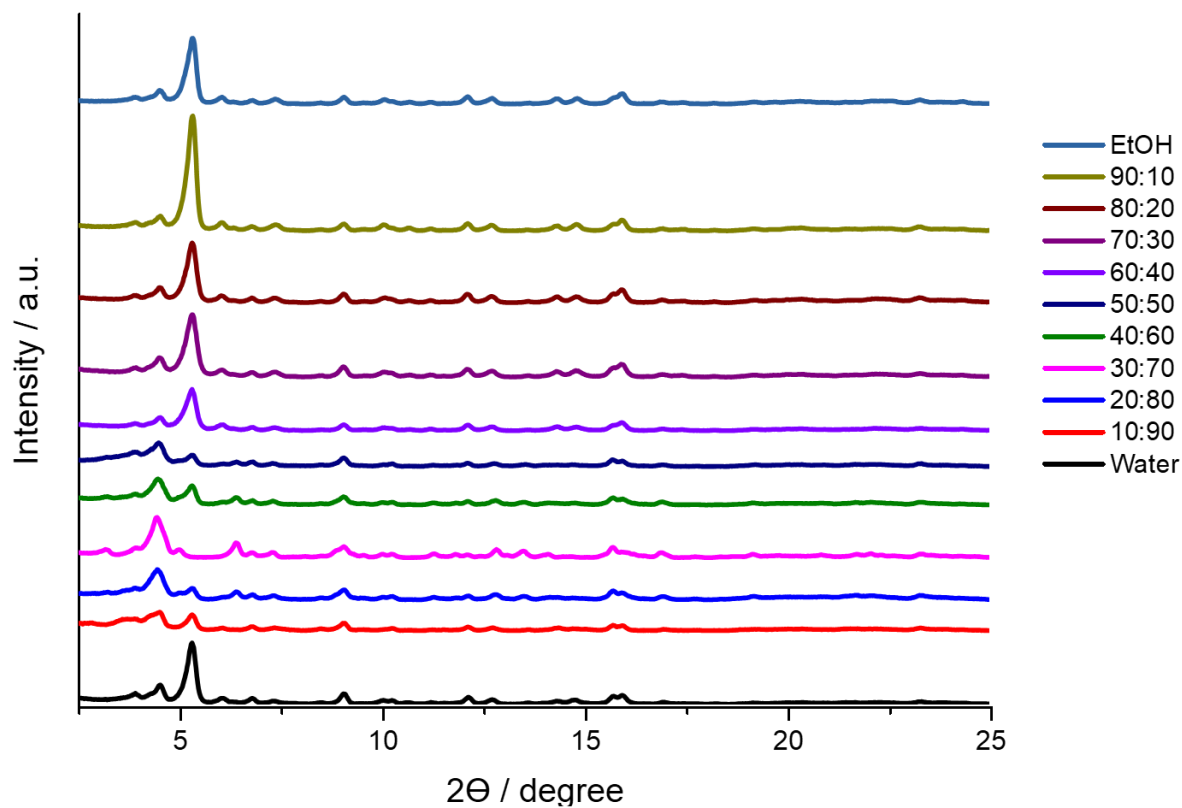


ESI Fig. 32 | Distribution histograms for M78BS-iPr xerogels width fibre dimensions from SEM images all at 10 mg/mL

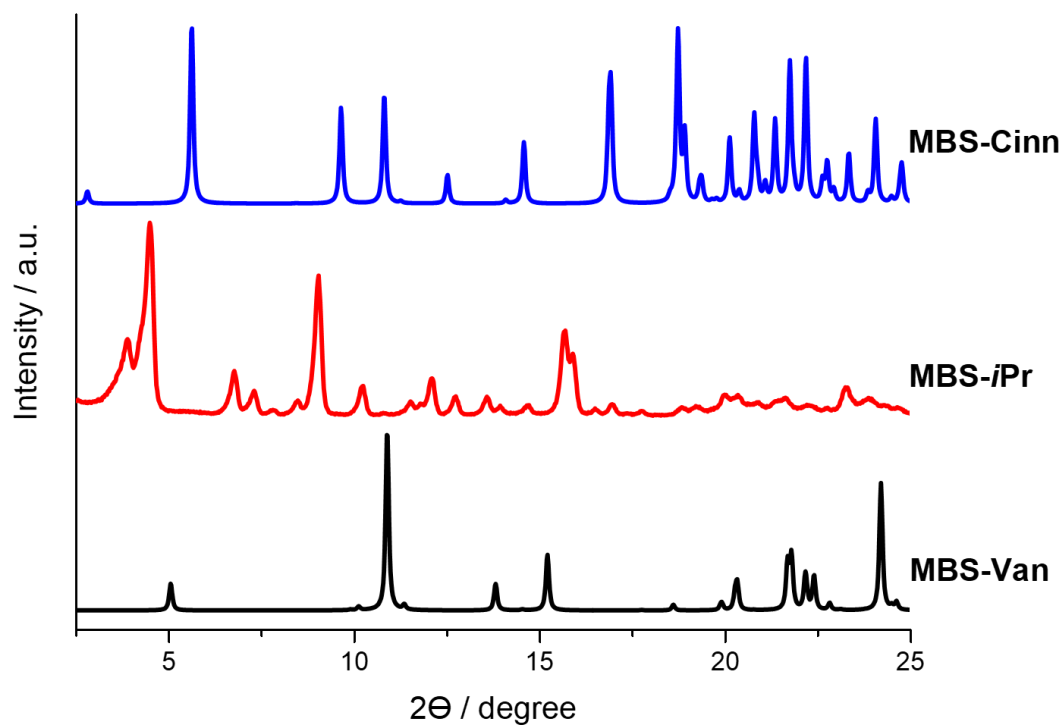


ESI Fig. 33 | SEM micrographs of equimolar xerogels formed in different solvents. All in 1% w/v upon heating and cooling. Conditions: xerogel prepared by drying the gel in air and then coating with 5nm IR before imaging under vacuum at 5kV. Scale bar in all images is 1 μm.

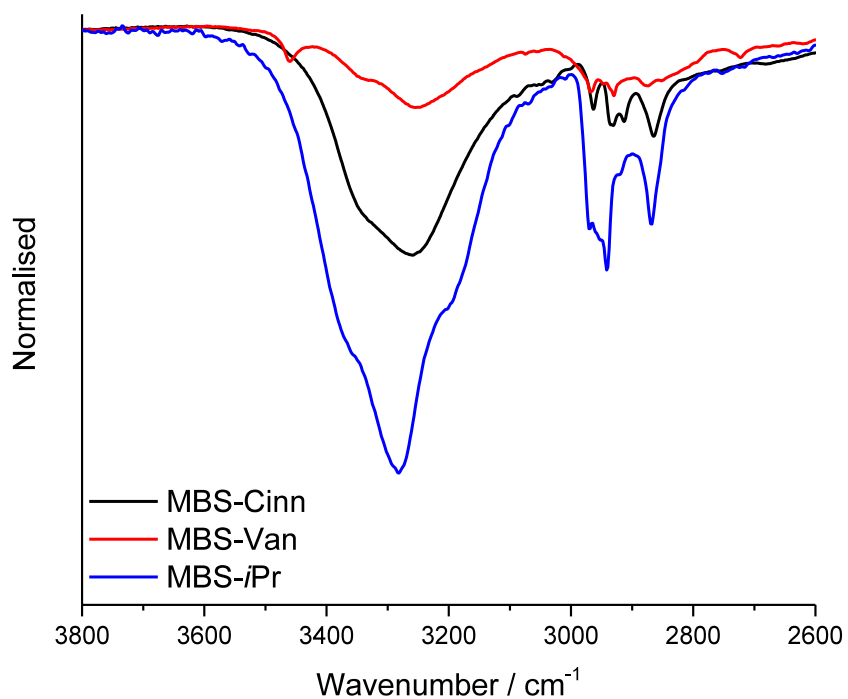
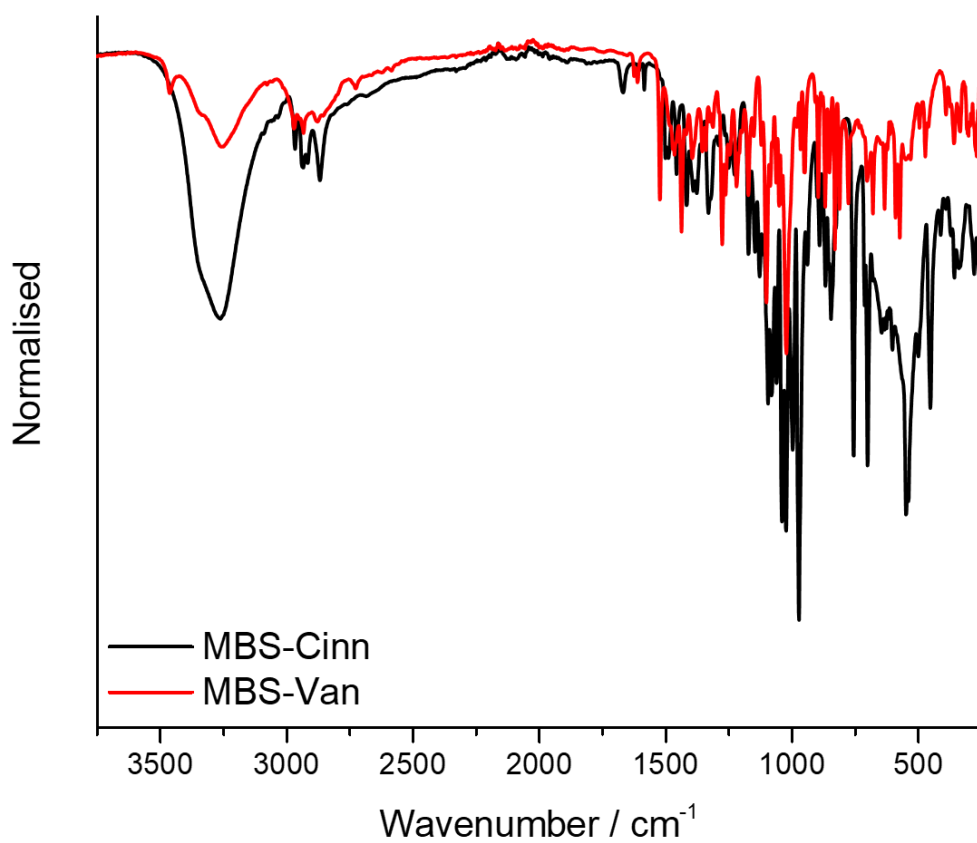
## Powder X-Ray Diffraction



ESI Fig. 34 | PXRD of equimolar xerogel made from all ethanolic/water solutions



ESI Fig. 35 | MBS-*i*Pr PXRD spectrum and the simulated PXRD of MBS-Cinn and MBS-Van from single crystal diffraction



ESI Fig. 36 | FTIR/ATR spectra of MBS-Cinn and MBS-Van Crystals (top) and an expansion showing the hydrogen bonding region compared with microcrystals of MBS-*i*Pr (bottom).

ESI Table 1 | Selected hydrogen bonding parameters

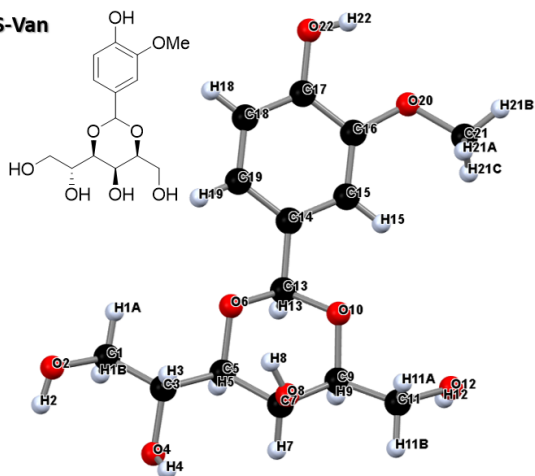
$D-H\cdots A$	$D-H$ (Å)	$H\cdots A$ (Å)	$D\cdots A$ (Å)	$D-H\cdots A$ (°)
<b>MBS-Cinn</b>				
O2A—H2A $\cdots$ O4B <sup>i</sup>	0.841	1.946	2.704 (11)	149.9
O8A—H8A $\cdots$ O8B	0.840	1.968	2.755 (10)	155.7
O8B—H8B $\cdots$ O4B <sup>ii</sup>	0.840	1.937	2.653 (10)	142.5
<b>MBS-Van</b>				
O2—H2 $\cdots$ O12 <sup>i</sup>	0.840	1.962	2.7898 (18)	168.3
O4—H4 $\cdots$ O8 <sup>iii</sup>	0.825 (19)	1.84 (19)	2.6531 (17)	165.1 (3)
O8—H8 $\cdots$ O4 <sup>iv</sup>	0.844 (19)	1.87 (2)	2.6649 (17)	155.9 (2)
O12—H12 $\cdots$ O2 <sup>v</sup>	0.83 (2)	1.93 (2)	2.7580 (19)	174.9 (3)

Symmetry code(s): (i)  $x-1, y+1, z$ ; (ii)  $x-1, y, z$ ; (iii)  $-x, y+1/2, -z+1$ ; (iv)  $x, y-1, z$ ; (v)  $x+1, y, z$ .

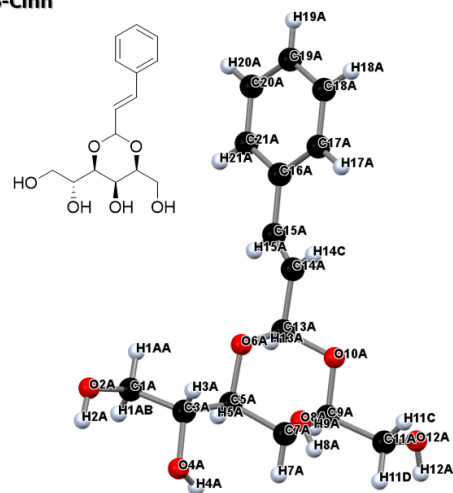
ESI Table 2 | Single crystal X-ray Experimental details

	MBS-Cinn	MBS-Van
Chemical formula	0.5(C <sub>15</sub> H <sub>20</sub> O <sub>6</sub> )-0.5(C <sub>15</sub> H <sub>18</sub> O <sub>6</sub> )	C <sub>14</sub> H <sub>20</sub> O <sub>8</sub>
<i>M<sub>r</sub></i>	296.31	316.30
Temperature (K)	120	120
Crystal system	Monoclinic	Monoclinic
Space group	<i>P</i> 2 <sub>1</sub>	<i>P</i> 2 <sub>1</sub>
<i>a</i> , <i>b</i> , <i>c</i> (Å)	4.7673 (11), 9.5601 (19), 31.386 (6)	8.92283 (14), 4.60123 (7), 17.4539 (3)
$\alpha$ , $\beta$ , $\gamma$ (°)	90, 92.31 (2), 90	90, 92.9088 (15), 90
<i>V</i> (Å <sup>3</sup> )	1429.3 (5)	715.66 (2)
<i>Z</i>	4	2
Radiation type	Cu <i>K</i> $\alpha$	Cu <i>K</i> $\alpha$
$\mu$ (mm <sup>-1</sup> )	0.89	1.03
Crystal size (mm)	0.27 × 0.03 × 0.02	0.20 × 0.05 × 0.03
Reflections collected	8745	9752
Independent reflections	4045	2828
Reflections [ <i>I</i> > 2 $\sigma$ ( <i>I</i> )]	2892	2777
<i>R</i> <sub>int</sub>	0.124	0.023
$\theta$ <sub>max</sub> (°)	58.9	73.5
(sin $\theta$ / $\lambda$ ) <sub>max</sub> (Å <sup>-1</sup> )	0.556	0.622
<i>R</i> [ <i>F</i> <sup>2</sup> > 2 $\sigma$ ( <i>F</i> <sup>2</sup> )], <i>wR</i> ( <i>F</i> <sup>2</sup> ), <i>S</i>	0.088	0.025
<i>wR</i> ( <i>F</i> <sup>2</sup> ) [all data]	0.224	0.067
Goodness-of-fit on <i>F</i> <sup>2</sup>	1.06	1.06
No. of reflections	4045	2828
No. of parameters	449	201
No. of restraints	697	7
Largest diff. Peak/hole (eÅ <sup>-3</sup> )	0.41, -0.28	0.21, -0.18
CCDC number	1945762	1945763

(a) MBS-Van

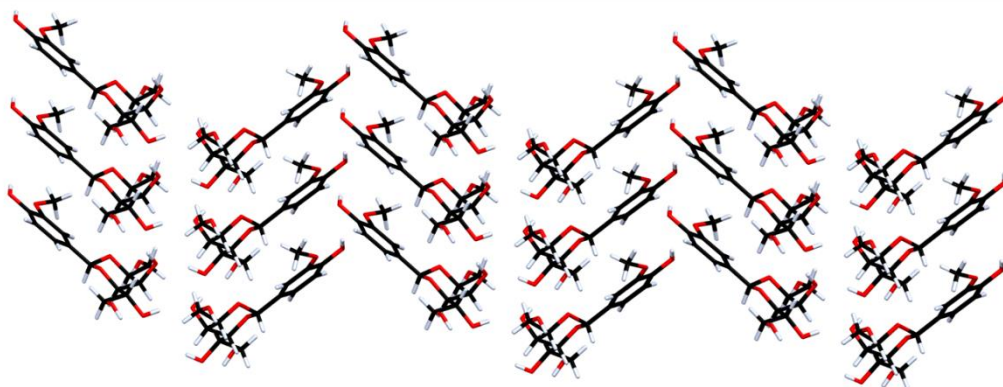


(b) MBS-Cinn

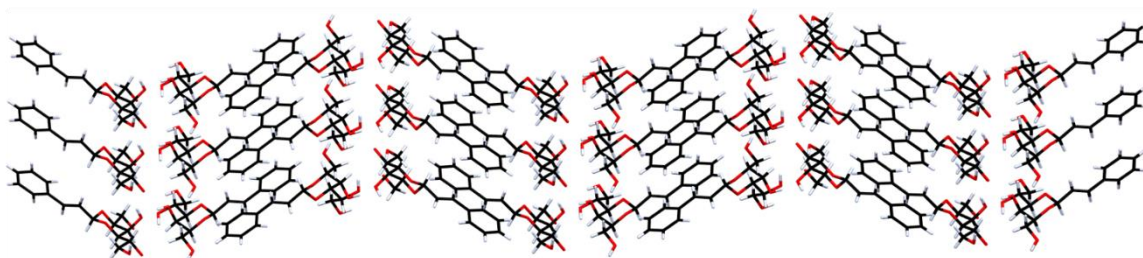


ESI Fig. 37 | Crystal structures of MBS-Van and MBS-Cinn

(a) MBS-Van

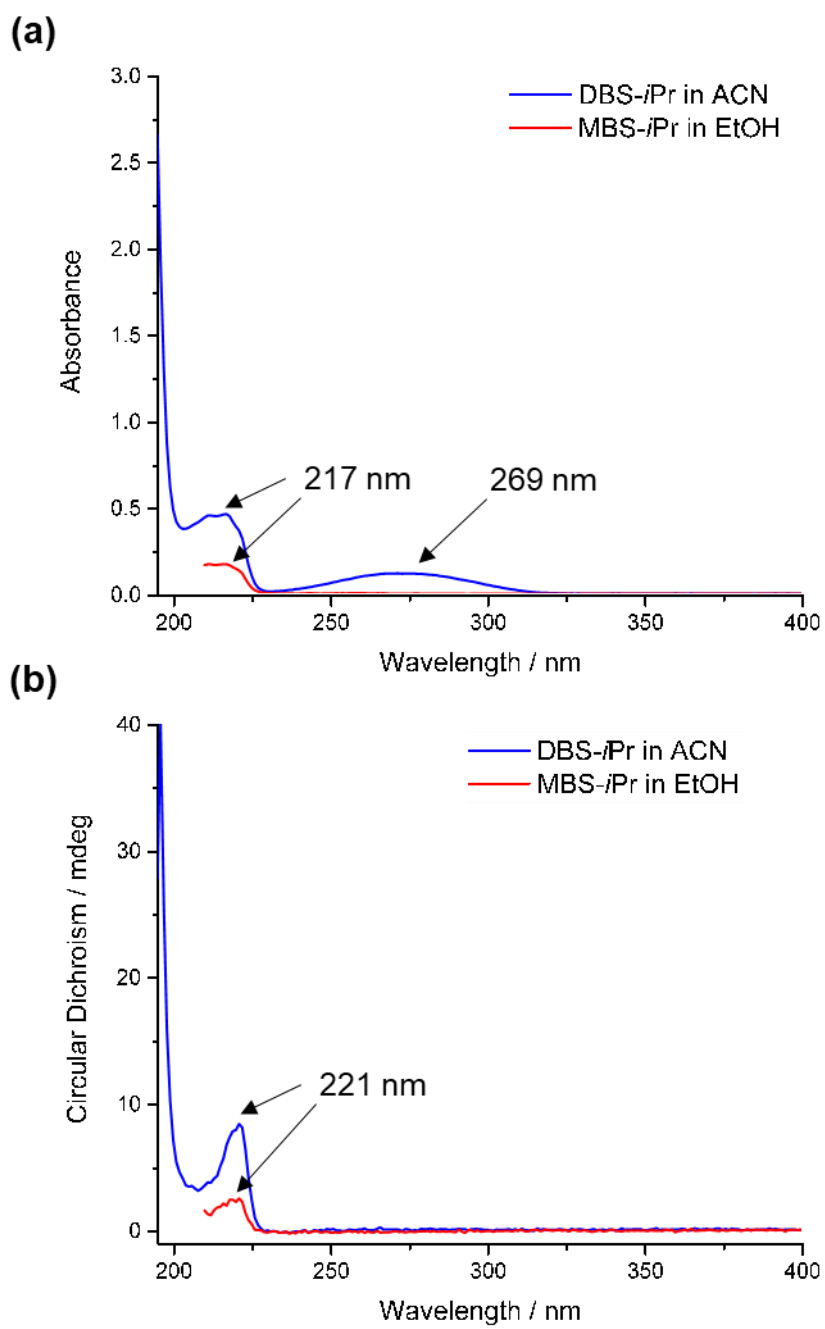


(a) MBS-Cinn



ESI Fig. 38 | Packing motifs of MBS-Van and MBS-Cinn

## Circular Dichroism



ESI Fig. 39 | (a) Absorbance and (b) circular dichroism spectra for DBS-*i*Pr in acetonitrile (blue) and MBS-*i*Pr in ethanol (red).

## References

- ESI1. J. Cosier and A. M. Glazer, *J. Appl. Crystallogr.*, 1986, 19, 105-107.
- ESI2. CrysAlisPro 1.171.40.45a (Rigaku OD, 2019).
- ESI3. O. V Dolomanov, L. J. Bourhis, R. J. Gildea, J. A. K. Howard, H. Puschmann, *J. Appl. Cryst.* 2009, 42, 339–341.
- ESI4. G. M. Sheldrick, *Acta Crystallogr. A* 2015, 71, 3–8.
- ESI5. G. M. Sheldrick, *Acta Crystallogr. C* 2015, 71, 3–8.
- ESI6. “CheckCIF,” can be found under <http://checkcif.iucr.org>